Invited Speaker

1180 Mechanics of blastocyst morphogenesis
Jean-Léon Maître

1178 Adding Dimensions to Intravital Imaging to Better Eavesdrop on Biology
Professor Scott Fraser[1,2]
[1]Vice President of Science Grant Programs, Chan-Zuckeberg Initiative, , , [2]Elizabeth Garrett Chair of Convergent Bioscience University of Southern California, ,

Oral Presentation

11 Digital Holographic Microscopy of Pseudomonas aeruginosa to Probe Effects of Membrane Active Antimicrobials
Mrs Elizabeth Ison[1,2], Dr Robert P Howlin[3], Dr Ricarda O Hawkins[3], Dr David J Bradshaw[3], Prof Paul Williams[2], Prof Morgan R Alexander[1]
[1]School of Pharmacy, University of Nottingham, Nottingham, United Kingdom, [2]BioDiscovery Institute, University of Nottingham, Nottingham, United Kingdom, [3]Haleon, Weybridge, United Kingdom

580 Novel tools for the Spatio-Temporal Photocontrol of protein-protein interactions
Dr Virginia Puente[1,2,3], Dr. Jan Tonnesen[3], Dr. Matthieu Sainlos[1]
[1]Interdiscipinary Institute for Neuroscience-IINS-CNRS, Bordeaux, France, [2]Faculty of Medicine-UPV/EHU, Leioa, Spain, [3]Biofika Center - CSIC, Leioa, Spain

670 A new transgenic mouse model for functional tracing of circulation via albumin-tagged fluorescent probes
Xiaowen Wang[1], Marta Vittani[1], Ashley Bomin Lee[1], Yuichi Hiraoka[2], Ayumu Konno[3,5], Philip Knak[1], Peter Kusk[1], Masaki Nagao[1], Miho Terunuma[4], Hirokazu Hirai[3,5], Maiken Nedergaard[1,6], Kohichi Tanaka[2], Hajime Hirase[1,6]
[1]Center for Translational Neuromedicine, University of Copenhagen, Copenhagen, Denmark, [2]Laboratory of Molecular Neuroscience, Medical Research Institute (MRI), Tokyo Medical and Dental University (TMDU), Tokyo, Japan, [3]Department of Neurophysiology and Neural Repair, Gunma University Graduate School of Medicine, Maebashi, Japan, [4]Division of Oral Biochemistry, Faculty of Dentistry & Graduate School of Medical and Dental Sciences, Niigata University, Niigata, Japan, [5]Viral Vector Core, Gunma University Initiative for Advanced Research, Maebashi, Japan, [6]Center for Translational Neuromedicine, University of Rochester Medical Center, Rochester, USA

690 Role of Miro1 adaptor protein in mitochondrial mobility between cancer and stromal cells
MSc. Jaromír Novák[1,2], Zuzana Nahacka[1], Gabriela Oliveira[1,3,4,5], Petra Brisudova[1,2], Sarka Dvorakova[1], Marketa Dalecka[2], Verena Puttrich[1], Lenka Grycova[1], Ludek Stepanek[6], Renata Zobalova[1], Mikkel Terp[7], Zdenek Lansky[1], Paulo Oliveira[3,4], Henrik Ditzel[7,8], Michael Berridge[9], Jakub Rohlena[1], Jiri Neuzil[1,2,10,11]
[1]Institute of Biotechnology, Czech Academy of Sciences, Vestec, Prague-West, Czech Republic, [2]Faculty of Science, Charles University, Prague, Czech Republic, [3]Center for Neuroscience and Cell Biology, University of Coimbra, Coimbra, Portugal, [4]Centre for Innovative Biomedicine and Biotechnology, University of Coimbra, Coimbra, Portugal, [5]Institute for Interdisciplinary Research, Doctorate Program in Experimental Biology and Biomedicine (PDBEB), University of Coimbra, Coimbra, Portugal, [6]Czech Center for Phenogenomics, Institute of Molecular Genetics, Czech Academy of Sciences, Vestec, Prague-West, Czech Republic, [7]Institute of Molecular Medicine, University of Southern Denmark, Odense, Denmark, [8]Department of Oncology, Odense University Hospital, Odense, Denmark, [9]Malaghan Institute of Medical Research, Wellington, New Zealand ,

[10]School of Pharmacy and Medical Science, Griffith University, Southport, Australia, [11]1st Faculty of Medicine, Charles University, Prague, Czech Republic

736 Mechanics of morphogenesis – The re-invention of cell sheet folding

Dr. Pierre Haas[1,2,3], Dr Steph Höhn[4]
[1]Max Planck Institute for the Physics of Complex Systems, Dresden, Germany, [2]Max Planck Institute of Molecular Cell Biology and Genetics, Dresden, Germany, [3]Center for Systems Biology Dresden, Dresden, Germany, [4]Department of Applied Mathematics and Theoretical Physics, Cambridge, United Kingdom

1170 CARS microscopy for studies in skin physiology and pharmacology

Professor Jonathan Brewer[1], PhD Irina Iachina[1], MA Lomholt[1], Kim Nielsen[2], Morten Ebbesen[1]
[1]University of Southern Denmark , Odense, Denmark, [2]Leo Pharma, Ballerup, Denmark

1133 FLIPs: Novel genetically encoded biosensors for polarization microscopy

Paul Miclea[1], Vendula Nagy Markova[1], Alexey Bondar[1,2,3], Alina Sakhi[4], Dr. Josef Lazar[1]
[1]First Faculty of Medicine, Charles University in Prague, Prague, Czechia, [2]Biological Center CAS, Budweis, Czechia, [3]University of South Bohemia, Budweis, Czechia, [4]Inst. of Organic Chemistry and Biochemistry CAS, Prague, Czechia

1137 INSIHGT - Scalable, Accessible, Homogeneous Deep Multiplexed Immunolabelling Platform for 3D Spatial Biology

Dr Hei Ming Lai[1,2], Mr Jacky Tin Shing Hung[2,3], Mr Juno Chun Ngo Yau[2], Mr King Ngai Chow[2], Mr Thomas Chun Yip Wong[2]
[1]Department of Chemical Pathology, The Chinese University of Hong Kong, Shatin, New Territories,, Hong Kong SAR, China, [2]Li Ka Shing Institute of Health Sciences, The Chinese University of Hong Kong, Shatin, New Territories,, Hong Kong SAR, China, [3]Department of Psychiatry, The Chinese University of Hong Kong, Shatin, New Territories,, Hong Kong SAR, China

Poster Presentation

24 The Best of Both Worlds: Combining Label Free and Fluorescence Imaging with Livecyte

Peter Djali[1], Dr Meetal Jotangia[1]
[1]Phase Focus Ltd, Sheffield, United Kingdom

207 Paleopalynology of Holocene birch hybridization in Iceland

Kesara Anamthawat-Jonsson[1]
[1]Institute of Life and Environmental Sciences, University of Iceland, Reykjavik, Iceland

310 Exploring the 3D architecture of native and stained human intervertebral discs through micro-CT

Raluca-Ana-Maria Barna[1,3,4], Federica Orellana[1,2], Marie-Rosa Fasser[4,5], Daniel Valent[4], Jonas Widmer[4,5], Annapaola Parrilli[1]
[1]Empa - Center for X-Ray Analytics, Dübendorf, Switzerland, [2]University of Fribourg, Fribourg, Switzerland , [3]University of Bern, , Switzerland, [4]Balgrist University Hospital - Spine Biomechanics, Zurich, Switzerland, [5]Balgrist University Hospital - Department of Orthopedics, Zurich, Switzerland

357 The effect of mesenchymal stem cell's secretome on hyperglycemia-related complications: focus on reproductive system disorders

Dr. Basak Isildar[1]
[1]Balikesir University Faculty of Medicine Histology and Embryology Department, Balıkesir, Türkiye

745 A new protocol for fluorescent quantitative labeling of individual proteins for live cell internalization assays

Dr Juan De Dios Alche[1,3], Dr. Alfonso Clemente[2], Dr. Antonio J. Castro[1]
[1]Department of Stress, Development and Signaling in Plants. Estacion Experimental del Zaidin. CSIC, Granada, Spain, [2]Department of Nutrition, Gastrointestinal Health and Food Safety. Estacion Experimental del Zaidin. CSIC, Granada, Spain, [3]University Institute of Research on Olive Grove and Olive Oils, Jaen, Spain

778 Exploring Cell-Material Interactions at Focal Adhesion Points
Dr Krzysztof Berniak[1], Dr Daniel P. Ura[1], Prof. Adam Piórkowski[2], Prof. Urszula Stachewicz[1]
[1]Faculty of Metals Engineering and Industrial Computer Science, AGH University of Krakow, Kraków, Polska, [2]Department of Biocybernetics and Biomedical Engineering, AGH University of Krakow, Kraków, Polska
783 Self-assembly of amphiphilic dendrimers investigated by standard, cryo and liquid TEM
Dr Tom ROUSSEL[1], Pr Ling PENG[1], Pr Suzanne GIORGIO[1]
[1]CINAM - CNRS- Aix Marseille University, Marseille, France
813 Fast nanoparticle passage over cell membrane identified using 3D STED cross-sectional imaging
Dr. Boštjan Kokot[1], Hana Kokot[1], Janez Štrancar[1]
[1]J. Stefan Institute, Ljubljana, Slovenia
830 Microscopic characterization of graphene derivates in life science
Mgr., Phd Zuzana Chaloupkova[1,2], Mgr. Jana Straska[1,2]
[1]Czech Advanced Technology and Research Institute - Regional Centre of Advanced Technologies and Materials, Olomouc, Czech Republic, [2]VSB Tech Univ Ostrava, IT4Innovations, Ostrava, Czech Republic
862 Birefringence analysis of hemozoin with surface plasmon microscopy towards malarial species distinction
Dr. Ipsita Chakraborty[1], Prof. Andreas Offenhäusser[1]
[1]Forschungszentrum Jülich GmbH, Jülich,, Germany
872 Microscopy of body surface sculpturing in terrestrial crustaceans
Ana Žuran[1], Dr. Miloš Vittori[1]
[1]Department of Biology, Biotechnical Faculty, University of Ljubljana, Ljubljana, Slovenia
902 Mechanisms of microglial responses to injury related focal ATP events
Dr Zsuzsanna Környei[1], Péter Berki[2,5,6], Dr Csaba Cserép[1], Dr Nikolett Lénárt[1], Dr Balázs Pósfai[1], Balázs Kalmár[1], Dr Kaikai He[3], Dr Ya Wang[4], Dr Zhaofa Wu[3], Dr Yulong LI[3], Dr Miao Jing[4], Dr Ádám Dénes[1]
[1]Momentum Laboratory of Neuroimmunology, Institute of Experimental Medicine, Budapest, Hungary, [2]János Szentágothai Doctoral School of Neuroscience, Semmelweis University, Budapest, Hungary, [3]State Key Laboratory of Membrane Biology, New Cornerstone Science Laboratory, School of Life Sciences, Peking University, Beijing , China, [4]Chinese Institute for Brain Research, Beijing , China, [5]Laboratory of Cerebral Cortex Research, Institute of Experimental Medicine, Budapest, Hungary, [6]Laboratory of Neuronal Network and Behaviour, Institute of Experimental Medicine, Budapest, Hungary
941 Mapping of phase separation of supramolecular protein assemblies by live-cell holotomography microscopy
Dr Orlando Marin[1], Dr Arina Dalaloyan[1], Professor Michael Elbaum[1]
[1]Weizmann Institute of Science, Rehovot, Israel
944 Enhanced sensitivity in label-free live-cell imaging using multi-pass stimulated Raman scattering microscopy
Joshua Reynolds[1], Dr. Shaun Burd[1], Tzu-Chieh (Jerry) Yen[1], Dr. Samsuzzoha Mondal[1,2], Dr. Soichi Wakatsuki[1,2], Dr. Mark Kasevich[1]
[1]Stanford University, Stanford, USA, [2]SLAC National Accelerator Laboratory, Menlo Park, USA
952 Temporal analysis of bone development in chick femur bone using label-free imaging
Miss Siddhi Chugh[1], Mr Jacob Kleboe[1,2], Dr Rahul S. Tare[3], Professor Richard OC Oreffo[2,3], Professor Sumeet Mahajan[1,2]
[1]School of Chemistry, Southampton, United Kingdom, [2]Institute of Life Sciences, Southampton, United Kingdom, [3]Human Development and Health, Southampton, United Kingdom
987 Non-toxic clearing and labeling with fluorescent REAfinityTM antibodies for enhanced 3D visualization of tissues
Msc Kevin Bigott[1]

[1]Miltenyi Biotec B.V. & Co. KG, Cologne, Germany

1040 Ex Vivo Metabolic Imaging for Parotid Tumors: Implications for Precise Diagnosis and Customized Treatment

Phd Student Alessia Riente[1,2], Dr Alessio Abeltino[1,2], Dr Cassandra Serantoni[1,2], Dr Michele Maria De Giulio[1,2], Dr Duaa Hatem[1,2], Prof Marco De Spirito[1,2], Dr Mariaconsiglia Santantonio[3], Dr Michela Sollazzo[2], Dr Lela Calò[2], Prof Giulio Cesare Passali[2], Dr Jacopo Galli[2], Prof Giuseppe Maulucci[1,2]

[1] Catholic University of the Sacred Heart, Rome, Italy, [2]Fondazione Policlinico Universitario A. Gemelli IRCCS, Rome, Italy, [3]Ospedale Pediatrico Bambino Gesù, Rome, Italy

1080 CAR T cell dynamics in a 3D collagen matrix: migration and interactions with cancer cells

Nicoline Dorothea Daugaard[1], Mike Bogetofte Barnkob[2], Zelvera Ismetova Usheva[2], Torben Barington[2], Jonathan R. Brewer[1]

[1]Department of Biochemistry and Molecular Biology, University of Southern Denmark, Odense, Denmark, [2]Centre for Cellular Immunotherapy of Haematological Cancer Odense (CITCO), Department of Clinical Immunology, Odense University Hospital, University of Southern Denmark, Odense, Denmark

1115 Investigating nanoparticle interactions with the human blood-brain barrier in vitro

Hakan Sahin[1], Oguz Yucel[2], Dr. Paul Holloway[3], Eren Yildirim[2], Dr. Serkan Emik[2], Dr. Gulten Gurdag[2], Dr. Gamze Tanriverdi[1], Dr. Gozde Erkanli Senturk[1]

[1]Department of Histology and Embryology, Cerrahpasa Faculty of Medicine, Istanbul University-Cerrahpasa, Istanbul, Turkey, [2]Department of Chemical Engineering, Faculty of Engineering, Istanbul University-Cerrahpasa, Istanbul, Turkey, [3]Radcliffe Department of Medicine, University of Oxford, Oxford, UK

1171 Exploring Melanoma Dynamics: Insights from a 3D Cell Culture Model with Vemurafenib Treatment

Rikke Tholstrup[1], Nicoine Dorothea Daugaard[1], Daniela De Zio[2], Jonathan Brewer[1]

[1]University of Southern Denmark, Odense, Denmark, [2]Danish Cancer Institute, Copenhagen, Denmark

Late Poster Presentation

1199 Transdifferentiation of human dental pulp-derived mesenchymal stem cells into neurospheres and transplantation into aganglionic hindgut

Msc Adam Soos[1], MSc. Emoke Szocs[1], Bendeguz Sramko[2], Anna Abbas[2], Dr. Anna Foldes[3], PhD Karolina Pircs[2], Prof. PhD. Nandor Nagy[1]

[1]Department of Anatomy, Histology and Embryology, Semmelweis University, Budapest, Hungary, [2]Institute of Translational Medicine, Semmelweis University, Budapest, Hungary, [3]Department of Oral Biology, Semmelweis University, Budapest, Hungary

1218 3D imaging, visualisation, and analysis services at Lund University Bioimaging Centre

Dr Sebastian Wasserstrom[1], Dr John Stegmayr[1], Dr Nils Norlin[1]

[1]Lund University Bioimaging Centre, Lund, Sweden

1260 Analysis of transcription dynamics via single cell imaging of chemically inducible system in S. Cerevisiae

Yujie Zhong[1], Maximilian Gehri[1], Gamze Dogali[1], Heinz Koeppl[1]

[1]Self-organizing Systems, Darmstadt, Germany

1351 3D Spatial Transcriptomics: A MERFISH Platform for High-Resolution Molecular Imaging

Postdoc Sofie Bendixen[1], PhD Jakob Tornby[1], Scientific Staff Morten Ebbesen[1], PhD Rikke Tholstrup[1], PhD Katharina Kaiser, Professor Jonathan Brewer[1]

[1]Department of Biochemistry and Molecular Biology, University of Southern Denmark, Odense, Denmark

1180

Mechanics of blastocyst morphogenesis

Jean-Léon Maître

LS-02 (1), Lecture Theater 4, august 26, 2024, 10:30 - 12:30

During pre-implantation development, the mammalian embryo forms the blastocyst. The architecture of the blastocyst is essential to the specification of the first mammalian lineages and to the implantation of the embryo. Consisting of an epithelium enveloping a fluid-filled lumen and the inner cell mass, the blastocyst is sculpted by a succession of morphogenetic events. These deformations result from the changes in the forces and mechanical properties of the tissue composing the embryo. Combining microscopy (spinning disk, light sheet and lattice light sheet confocal microscopy), image analysis, biophysical tools (such as optical tweezers) and genetics, we study the mechanical and cellular changes leading to the formation of the blastocyst.

1178

Adding Dimensions to Intravital Imaging to Better Eavesdrop on Biology

Professor Scott Fraser[1,2]
[1]Vice President of Science Grant Programs, Chan-Zuckeberg Initiative, , , [2]Elizabeth Garrett Chair of Convergent Bioscience University of Southern California, ,

LS-02 (2), Lecture Theater 4, august 26, 2024, 14:00 - 15:00

Imaging of living specimens can animate the wealth of high-throughput molecular data to better understand complex events ranging from embryonic development to disease processes. We are advancing this approach despite the unavoidable tradeoffs - between spatial & temporal resolution, field of view, limited photon budget - by constructing faster and more efficient light sheet and laser-scanning microscopes that maintain subcellular resolution.
Our two-photon light-sheet microscope combines the deep penetration of two-photon microscopy and the speed of light sheet microscopy to generate images with more than 10x improved imaging speed & sensitivity. Better engineering of the detection objective's point-spread-function improves this another 3-fold. Two-photon excitation light is far less scattered, permitting subcellular resolution to be maintained better than conventional light sheet microscopes, resulting in 4D (3D over time) cell and molecular imaging with sufficient speed and resolution to unambiguous trace cell lineages, movements and signals in intact systems.
To increase the 5th Dimension (# of simultaneous labels), we are refining new multispectral image analysis tools that exceed the performance of our previous work on Linear Unmixing by orders of magnitude in speed, error propagation and accuracy. Novel denoising strategies using machine learning permit imaging at far lower light levels, yielding rapid and unambiguous analyses without perturbing even fragile multiplex-labeled specimens.
Parallel refinements in label-free approaches extend imaging to patient-derived tissues and even human subjects. The low concentrations of these intrinsic labels required us to refine fluorescence lifetime imaging (FLIM), and combine it with multispectral and advanced denoising tools, to perform intravital imaging in such challenging settings.
Combined, these imaging and analysis tools offer the multi-dimensional imaging required to follow key events in intact systems as they take place, and allow us to use noise and variance as experimental tools rather than experimental limitations.

11

Digital Holographic Microscopy of Pseudomonas aeruginosa to Probe Effects of Membrane Active Antimicrobials

Mrs Elizabeth Ison[1,2], Dr Robert P Howlin[3], Dr Ricarda O Hawkins[3], Dr David J Bradshaw[3], Prof Paul Williams[2], Prof Morgan R Alexander[1]
[1]School of Pharmacy, University of Nottingham, Nottingham, United Kingdom, [2]BioDiscovery Institute, University of Nottingham, Nottingham, United Kingdom, [3]Haleon, Weybridge, United Kingdom

LS-02 (1), Lecture Theater 4, august 26, 2024, 10:30 - 12:30

Background: Digital holographic microscopy (DHM) is a unique label-free imaging technique that allows interrogation of a population of individual bacterial trajectories in 3D. An inline-holography approach was taken to discern the effect of the antimicrobial compounds on the motility of the bacterium, Pseudomonas aeruginosa. Bacterial swimming motility depends on membrane-embedded stators that couple an electrochemical gradient with the mechanical rotation of the flagellum. Hence, there is a tight link between the bacterial membrane and motility. We propose that this allows us to use 3D motility changes of P. aeruginosa as a proxy of membrane damage over time, which test by following changes in antimicrobial susceptibility as a function of the bacterial growth phase. Susceptibility to antimicrobials as the upregulation of the alternative sigma factor rpoS could increase resistance as the bacteria enter the stationary growth phase. Antimicrobials were adsorbed to surfaces, exposed to bacteria, and monitored for changes in motility.
Aim: To discern the effects of antimicrobial adsorbed surfaces on bacterial motility using DHM and test whether this links to membrane damage.
Methods: To demonstrate desorption of antimicrobials (chlorhexidine (CHX), cetylpyridinium chloride (CPC), 4-isopropyl-3-methylphenol (IPMP) and formulated (f-CHX)) from the adsorbed surfaces, they were exposed to constitutive light emitting P. aeruginosa CTX::tac'-luxCDABE. Any reduction in bioluminescence is indicative of membrane damage consistent with antimicrobial desorption. The motility profiles of both exponential and stationary growth phase wild type (WT) and rpoS mutant were visualised using DHM with 1000 frame (18 s) image streams being taken every 10 min over 1 h. A 685 nm laser illumination was used and a 20x/0.75 NA objective. Bacteria were tracked using bespoke LABVIEW scripts and reconstructed using MATLAB.
Results: Bioluminescence from the constitutive light emitting P. aeruginosa CTX::tac'-luxCDABE decreased over time with CHX and f-CHX exposure for WT and rpoS cells in both the exponential and stationary growth phase. This corresponded with changes in bacterial trajectories when cells were exposed to CHX and f-CHX which showed increased numbers of sharp turns, quantified as an increase in tortuosity. Stationary WT cells only responded to f-CHX adsorbed surfaces but displayed similar changes in motility. The rpoS mutants displayed increased tortuosity with CHX at both early exponential phase and stationary phase of growth. CPC and IPMP showed no change in luminescence (no deleterious membrane impact) and no change in tortuosity at the concentrations tested.
Conclusions: CHX and f-CHX readily desorb from surfaces, dissipating membrane potential which in turn impacts on bacterial motility. The rpoS gene is important for P. aeruginosa resistance to adsorbed CHX. These motility changes could be discerned through the label-free DHM technique.

Keywords:

Holography, Microbiology, Motility

580

Novel tools for the Spatio-Temporal Photocontrol of protein-protein interactions

Dr Virginia Puente[1,2,3], Dr. Jan Tonnesen[3], Dr. Matthieu Sainlos[1]
[1]Interdiscipinary Institute for Neuroscience-IINS-CNRS, Bordeaux, France, [2]Faculty of Medicine-UPV/EHU, Leioa, Spain, [3]Biofika Center - CSIC, Leioa, Spain

LS-02 (1), Lecture Theater 4, august 26, 2024, 10:30 - 12:30

Background incl. aims
The dynamic regulation of AMPA glutamate receptors (AMPARs) trafficking into and out of the synapse is a major mechanism underlying synaptic plasticity, a fundamental basis of learning and memory. However, the detailed molecular mechanisms governing the dynamics of these postsynaptic receptors are still not fully understood, stressing the need for new methods to modulate and monitor these processes. With the purpose of controlling locally, acutely and in a reversible manner the interaction between proteins involved in AMPAR trafficking we have developed original biomolecular tools based on optogenetics. These approaches will be effectively applied with spatial and temporal precision on selectively targeted individual cells and they will work based on two strategies: by reversibly immobilizing proteins by light, or light-controlling the binding state (association / dissociation) of proteins. The design and production of these tools have involved molecular/cell biology, biochemistry and protein engineering for later on, validating them in heterologous cells and neurons by Advanced Fluorescence Techniques. Our tools effectively address current technical limitations in neuroscience and could allow investigating questions from further biological disciplines.

Methods
The design and production of these optotools have involved molecular/cell biology, protein engineering and biophysical characterization, for later on, validated them in heterologous cells by Advanced Fluorescence Techniques. In order to characterize these approaches in transfected eukaryotic cells as a model of complex cellular context, a new red shifted FRET pair has been developed to monitor protein interactions. Besides heterologous cells, the approaches have been also validated by u-PAINT in neurons.

Results
On one hand, we have designed Photoactivatable competing ligands to destabilize AMPARs by disruption of the natural interaction between Stargazin and PSD-95. On the other hand, we have engineered photoswitchable crosslinkers to specifically recognize AMPAR subunits and control with spatio-temporal resolution the mobility and local number of AMPARs.

Conclusions
The approaches we have engineered should most importantly allow tackling fundamental questions related to AMPARs mobility but also be of high impact on a large scientific community as they could be transferable to many systems.

Keywords:

Optogenetics, super resolution, FLIM-FRET, PPI,

Reference:

- Zohu et al. Science. 2012, 338, 810-814
-Taslimi et al. Nat. Commun. 2014, 5:4925
- Grusch et al. EMBO J. 2014, 33(15):1713-26
- Beharry et al. Chem.Soc.Rev. 2011, 40, 4422-4437
- Wang et al. Nature Meth. 2016, 13, 755–758
- Sainlos et al. Nat. Chem. Biol. 2011, 7 (2) 81-91
- Sainlos et al. J.Am. Chem. Soc. 2013, 135 (12) 4580-4583
- Sainlos et al. J.Am. Chem. Soc. 2009, 131 (19) 6680-6682
- Bard et al. PNAS 2010, 107 (45) 19561-19566

670

A new transgenic mouse model for functional tracing of circulation via albumin-tagged fluorescent probes

Xiaowen Wang[1], Marta Vittani[1], Ashley Bomin Lee[1], Yuichi Hiraoka[2], Ayumu Konno[3,5], Philip Knak[1], Peter Kusk[1], Masaki Nagao[1], Miho Terunuma[4], Hirokazu Hirai[3,5], Maiken Nedergaard[1,6], Kohichi Tanaka[2], Hajime Hirase[1,6]

[1]Center for Translational Neuromedicine, University of Copenhagen, Copenhagen, Denmark, [2]Laboratory of Molecular Neuroscience, Medical Research Institute (MRI), Tokyo Medical and Dental University (TMDU), Tokyo, Japan, [3]Department of Neurophysiology and Neural Repair, Gunma University Graduate School of Medicine, Maebashi, Japan, [4]Division of Oral Biochemistry, Faculty of Dentistry & Graduate School of Medical and Dental Sciences, Niigata University, Niigata, Japan, [5]Viral Vector Core, Gunma University Initiative for Advanced Research, Maebashi, Japan, [6]Center for Translational Neuromedicine, University of Rochester Medical Center, Rochester, USA

LS-02 (1), Lecture Theater 4, august 26, 2024, 10:30 - 12:30

Liver-secreted albumin is the most abundant protein in blood plasma and cerebrospinal fluid. We have previously developed liver-targeting adeno-associated viral vectors (AAV8-P3-*) that express fluorescent protein-tagged albumin to visualize blood plasma in adult mice (DOI: 10.1016/j.crmeth.2022.100302). We have also established a virally induced CRISPR/Cas9-based knock-in of green fluorescent albumin in neonatal mice (DOI: 10.1101/2023.07.10.548084). Here, we have generated a new transgenic mouse model by CRISPR/Cas9 in which the bright red fluorescent protein mScarlet is knocked into the albumin locus to produce mScarlet-tagged albumin (Alb-mSc). In adult heterozygous knock-in mice, the plasma fluorescence signal intensity recorded an order of magnitude higher than a standard AAV-expressed Alb-mSc (AAV8-P3-Alb-mSc, 2E11 vg). This strong plasma fluorescence allowed for the imaging of the entire depth of the cortical vasculature reaching to the white matter (up to ~1mm in depth) by two-photon microscopy. Thin skull preparation enabled the visualization of dura mater by “shadow imaging”, where Alb-mSc presumably infiltrated into the interstitial space from dural vessels. Furthermore, Alb-mSc mice were crossed with Prox1-eGFP mice to delineate lymphatic structures. Alb-mSc signals were subdural interstitial space were clearly attenuated reflecting the composition of cerebrospinal fluid. Nonetheless, shadow imaging was possible in the cortical parenchyma, whereby cortical neurons are detected by the relatively high fluorescence of the extracellular space. The knock-in mouse line offers multi-purpose utilities for studying morphological and functional changes in the brain and other organs.

Keywords:

Circulation, Vasculature, Blood flow, Albumin

Reference:

Wang X, Delle C, Asiminas A, Akther S, Vittani M, Brøgger P, Kusk P, Vo CT, Radovanovic T, Konno A, Hirai H, Fukuda M, Weikop P, Goldman SA, Nedergaard M, Hirase H. Liver-secreted fluorescent blood plasma markers enable chronic imaging of the microcirculation. Cell Rep Methods. 2022 Sep 21;2(10):100302. doi: 10.1016/j.crmeth.2022.100302. PMID: 36313804; PMCID: PMC9606131.

Vittani M, Knak PAG, Fukuda M, Nagao M, Wang X, Kjaerby C, Konno A, Hirai H, Nedergaard M, Hirase H. Virally induced CRISPR/Cas9-based knock-in of fluorescent albumin allows long-term visualization of cerebral circulation in infant and adult mice. bioRxiv [Preprint]. 2023 Jul 10:2023.07.10.548084. doi: 10.1101/2023.07.10.548084. PMID: 37503027; PMCID: PMC10369863.

690

Role of Miro1 adaptor protein in mitochondrial mobility between cancer and stromal cells

MSc. Jaromír Novák[1,2], Zuzana Nahacka[1], Gabriela Oliveira[1,3,4,5], Petra Brisudova[1,2], Sarka Dvorakova[1], Marketa Dalecka[2], Verena Puttrich[1], Lenka Grycova[1], Ludek Stepanek[6], Renata Zobalova[1], Mikkel Terp[7], Zdenek Lansky[1], Paulo Oliveira[3,4], Henrik Ditzel[7,8], Michael Berridge[9], Jakub Rohlena[1], Jiri Neuzil[1,2,10,11]

[1]Institute of Biotechnology, Czech Academy of Sciences, Vestec, Prague-West, Czech Republic, [2]Faculty of Science, Charles University, Prague, Czech Republic, [3]Center for Neuroscience and Cell Biology, University of Coimbra, Coimbra, Portugal, [4]Centre for Innovative Biomedicine and Biotechnology, University of Coimbra, Coimbra, Portugal, [5]Institute for Interdisciplinary Research, Doctorate Program in Experimental Biology and Biomedicine (PDBEB), University of Coimbra, Coimbra, Portugal, [6]Czech Center for Phenogenomics, Institute of Molecular Genetics, Czech Academy of Sciences, Vestec, Prague-West, Czech Republic, [7]Institute of Molecular Medicine, University of Southern Denmark, Odense, Denmark, [8]Department of Oncology, Odense University Hospital, Odense, Denmark, [9]Malaghan Institute of Medical Research, Wellington, New Zealand , [10]School of Pharmacy and Medical Science, Griffith University, Southport, Australia, [11]1st Faculty of Medicine, Charles University, Prague, Czech Republic

LS-02 (1), Lecture Theater 4, august 26, 2024, 10:30 - 12:30

Background

Cancer cells are in close contact with healthy tissue to maintain proliferation and secure the protumorigenic microenvironment. An example of this intimate interaction is the ability of cancer cells to 'steal' functional mitochondria from surrounding stromal cells to compensate for damage to their own organelles, whether resulting from mutational burden or therapy intervention. This process, called horizontal mitochondrial transfer (HMT), occurs mostly via tunneling nanotubes (TNTs), thin membranous protrusions that connect the cytoplasm of donor and acceptor cell. Mitochondria move between cells over a distance of tens to hundreds of micrometres of TNT length using a microtubule-associated molecular adaptor and motor proteins. Here, we aim to elucidate the role of Miro1, an adaptor protein that is located in the outer mitochondrial membrane and is known to be involved in mitochondrial mobility and the HMT.

Methods

To elucidate the role of Miro1 in HMT in vivo, we have developed a mouse with inducible Miro1 knockout (Miro1KO) and with endogenous expression of the mitochondrial targeted mKate2 red fluorescence protein (mito::mKate2). We subcutaneously injected syngenic GFP expressing B16 cancer cells lacking mitochondrial DNA (so called ρ0 cells), representing a model of severe mitochondrial damage. This allows us to follow tumor growth with respect to Miro1 expression and identify HMT based on the presence of mito::mKate2 (stromal origin) mitochondria in GFP (ρ0 cancer cells) in vivo and in vitro. To further elucidate the role of Miro1 in cancer and stromal cells, we have used live cell time-lapse microscopy to capture the dynamics of mitochondrial movement as well as Sholl analysis to describe their location within cells. Finally, we have optimized cell-free reconstituted system of isolated microtubules, mitochondria, adaptor, and motor proteins, allowing us in combination with interference reflectance microscopy to track and identify alternations in movement of single organelles along microtubules.

Results

First, in vivo we observed a delay in mtDNA acquisition and tumor growth in Miro1KO mice. Furthermore, we elucidated that Miro1 is necessary for microtubule-mediated mobility and organelle relocalization toward the cell periphery and into TNTs. At the molecular level, our data suggest that Miro1 is necessary for the initial phase of mitochondrial movement, the association of organelles with microtubular tracks.

Conclusions

In summary, our results illustrate the importance of mitochondrial transfer in the context of cancer cells experiencing mitochondrial damage (e.g. as result of mutations or treatment). In particular, we have elucidated the role of Miro1 in this process, supporting the model in which it recruits mitochondria on microtubules, secures their movement towards the cell periphery and inside TNTs, and ultimately into the recipient cancer cell.

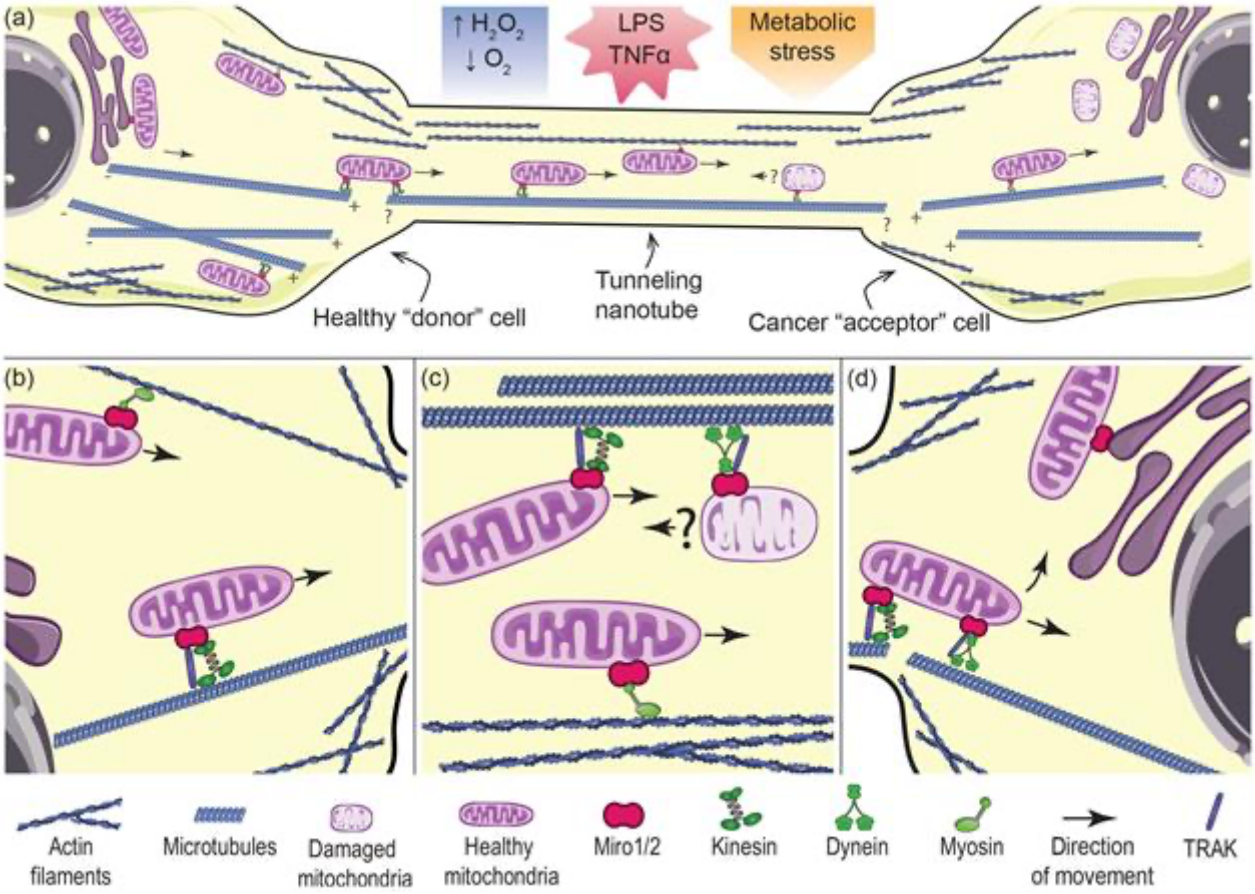

Keywords:

Horizontal mitochondrial transfer, Miro1, cancer

736

Mechanics of morphogenesis – The re-invention of cell sheet folding

Dr. Pierre Haas[1,2,3], Dr Steph Höhn[4]
[1]Max Planck Institute for the Physics of Complex Systems, Dresden, Germany, [2]Max Planck Institute of Molecular Cell Biology and Genetics, Dresden, Germany, [3]Center for Systems Biology Dresden, Dresden, Germany, [4]Department of Applied Mathematics and Theoretical Physics, Cambridge, United Kingdom

LS-02 (1), Lecture Theater 4, august 26, 2024, 10:30 - 12:30

Mechanical constraints impact the way that organs and tissues develop. Yet, we are only beginning to understand the physical principles that shape tissues. The folding of cellular monolayers, as seen in gastrulation, neurulation and organogenesis, serves as a model for understanding the shaping of three-dimensional tissues. Within the algal family Volvocaceae a range of complexity in cell sheet folding has evolved only 200MYA, providing an excellent model system to study the underlying mechanics. Volvox globator embryos consist of a spherical cellular monolayer which turns itself inside-out in a gastrulation-like process called inversion.
We have been using a combination of advanced light sheet and 2-photon time lapse imaging, biophysical perturbations, and mathematical modelling to understand the forces underlying inversion. We found that different ways to turn a sphere inside out have evolved in different volvocacean species, corresponding to deviations in geometrical constraints [1-4]. We have developed a framework to predict out-of-plane forces in dynamic three-dimensional cell sheets. Model-based analyses of orthogonal laser ablations allow us to infer out-of-plane forces and stresses (Fig. 1). [5]. We found that inversion is driven by spatio-temporally concerted changes in cell shapes, cell connections, and tissue properties. Our findings suggest that these green algae have likely evolved mechano-chemical signalling mechanisms, equivalent to those found in the animal kingdom.

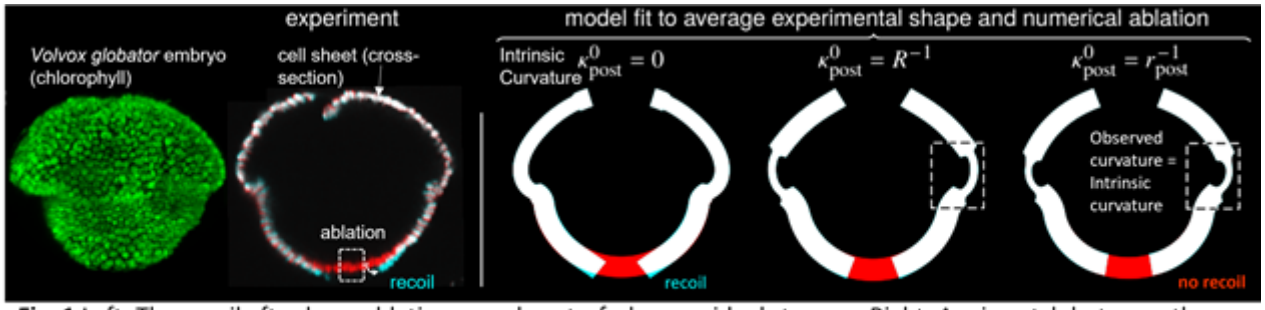

Fig. 1 Left: The recoil after laser ablation reveals out-of-plane residual stresses. Right: A mismatch between the observed curvature $\kappa = r^{-1}$ and the intrinsic curvature $\kappa^0 = 0$ causes these stresses and a recoil upon ablation.

Keywords:

Morphogenesis, mechanobiology, lightsheet-imaging, Volvox inversion

Reference:

[1] S.S. Höhn and A. Hallmann, BMC Biology 9, 89 (2011).
[2] S.S. Höhn, Honerkamp-Smith AR, Haas PA, Khuc Trong P, and Goldstein RE. Physical Review Letters 114, 178101 (2015).
[3] S.S. Höhn and A. Hallmann, BMC Developmental Biology, 16, (2016).
[4] P.A. Haas, S.S. Höhn, A.R. Honerkamp-Smith AR, J.B. Kirkegaard, and R.E. Goldstein. PLOS Biology 16, e2005536 (2018).
[5] S.S. Höhn and P.A. Haas, BioRxive, https://www.biorxiv.org/content/10.1101/2023.10.17.562736v1

1170

CARS microscopy for studies in skin physiology and pharmacology

Professor Jonathan Brewer[1], PhD Irina Iachina[1], MA Lomholt[1], Kim Nielsen[2], Morten Ebbesen[1]
[1]University of Southern Denmark , Odense, Denmark, [2]Leo Pharma, Ballerup, Denmark

LS-02 (1), Lecture Theater 4, august 26, 2024, 10:30 - 12:30

The application of Coherent anti-Stokes Raman Scattering (CARS) microscopy in biomedical research represents an extension in our ability to study complex biological systems with unique resolution and specificity. This presentation highlights the use of CARS microscopy to explore various aspects of skin physiology and pharmacology, demonstrating the technique's versatility and its potential to extend our understanding of biological tissues and treatment efficacy.
Firstly, utilizing CARS microscopy enabled the direct observation of time-dependent, spatially resolved diffusion of water (D2O) within human skin tissue, unveiling significant variations in diffusion coefficients across different strata of the Stratum Corneum (SC). This heterogeneity challenges the prevailing notion of the SC as a monolithic barrier, instead positing it as a complex, layered defense mechanism. This study show CARS microscopy's ability to quantitatively measure diffusion coefficients at varying tissue depths and locations.
Further, the examination of dissolvable microneedles for transdermal drug delivery underlines CARS microscopy's unique ability to visualize penetration of the microneedles and follow their morphology within the skin. By providing detailed images of microneedle degradation and drug dispersion, CARS microscopy offers valuable insights into the mechanisms of drug release and absorption, supporting the development of more effective transdermal therapeutics.
Additionally, employing CARS microscopy in conjunction with a perspiring skin simulator to assess sunscreen substantivity offers a novel approach to studying the interaction between topical formulations and physiological processes like sweating. This application highlights the technique's potential to dynamically follow the redistribution of specific active ingredients in the sunscreen during perspiration. Thus, evaluate product performance under realistic conditions, informing the design of more resilient and effective sunscreens.
Overall, these studies exemplify the power of CARS microscopy to provide detailed, molecule-specific insights into complex molecular interactions in tissue.

Keywords:

CARS, Drug delivery, Micro needles

Reference:

les for transdermal drug delivery showing skin pentation and modified drug release. European Journal of Pharmaceutical Sciences. 2023;182.
2. Iachina I, Lomholt MA, Eriksen JH, Brewer JR. Multilayer diffusion modeling and coherent anti-Stokes Raman scattering microscopy for spatially resolved water diffusion measurements in human skin. Journal of Biophotonics. 2022;15(10).
3. Keshavarzi F, Østergaard Knudsen N, Brewer JR, Ebbesen MF, Mirmahdi Komjani N, Zajforoushan Moghaddam S, et al. In vitro skin model for characterization of sunscreen substantivity upon perspiration. International Journal of Cosmetic Science. 2021;43(3):359-71.

1133

FLIPs: Novel genetically encoded biosensors for polarization microscopy

Paul Miclea[1], Vendula Nagy Markova[1], Alexey Bondar[1,2,3], Alina Sakhi[4], Dr. Josef Lazar[1]
[1]First Faculty of Medicine, Charles University in Prague, Prague, Czechia, [2]Biological Center CAS, Budweis, Czechia, [3]University of South Bohemia, Budweis, Czechia, [4]Inst. of Organic Chemistry and Biochemistry CAS, Prague, Czechia

LS-02 (2), Lecture Theater 4, august 26, 2024, 14:00 - 15:00

Background
Genetically encoded fluorescent biosensors convert specific biomolecular events into optically detectable signals. Typically, such probes utilize a suitable fluorescence quenching process in order to modulate the absorption or emission spectrum the fluorophore, or the fluorophore's lifetime. However, an unrelated detection principle, directionality of optical properties of fluorescent molecules, should also allow development of genetically encoded biosensors. Remarkably, despite numerous potential advantages of such biosensors (ratiometric readout, resistance to bleaching artifacts, information about protein structure, possibility of multiplexing, orthogonality to other approaches), optical directionality has remained largely unexploited as a detection principle. Our goal was to make optical directionality of fluorescent molecules widely applicable to imaging of biomolecular processes of cell signaling.

Methods
Using techniques of molecular biology, we set out to develop a series of genetically encoded biosensors suitable for observations of molecular processes of cell signaling by polarization-resolved fluorescence microscopy.

Results
We have now identified a novel design of genetically encoded fluorescent biosensors, which we term FLIPs(1,2,3) (Fluorescence anisotropy and LInear dichroism Probes). FLIPs offer an extremely simple design, high sensitivity, multiplexing capability, ratiometric output and resilience to bleaching artifacts. Importantly, FLIPs allow their targets to remain non-modified. The probes are applicable to imaging cellular activity of G protein coupled receptors, G proteins, arrestins, receptor tyrosine kinases and other signaling proteins, using simple microscopy instrumentation. The sensitivity of the probes allows even imaging of endogenously expressed targets.

Conclusion
The simplicity, modularity and versatility of the FLIP design allows rapid creation of biosensors of desirable properties. By exploiting a simple, universal, yet long overlooked detection principle, FLIPs open a wide new area of development both in genetically encoded fluorescent biosensors and in optical instrumentation.

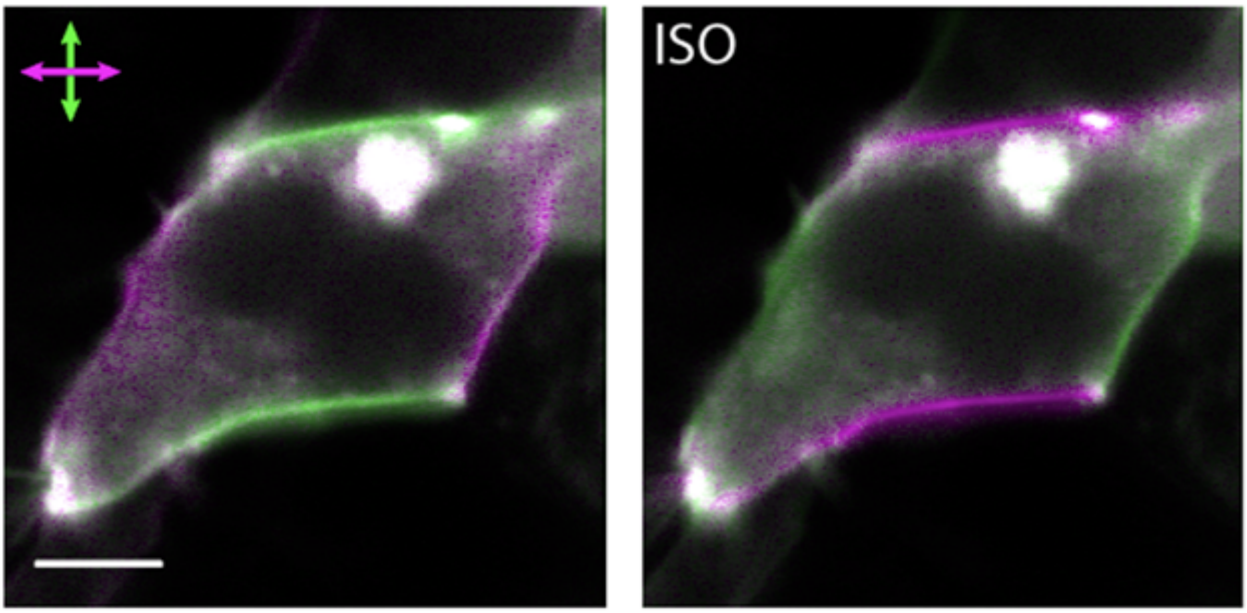

Keywords:

Polarization microscopy, biosensors, GPCR signaling

Reference:

1) Miclea P., Nagy Markova V., Bondar A., Sakhi A., Lazar J.; Novel Genetically Encoded Biosensors for Functional Imaging of Cell Signaling by Polarization Microscopy; https://www.biorxiv.org/content/10.1101/2024.02.23.581811v2
2) Lazar J., Bondar A., EPO patent application 21209717.4
3) 'FLIP' and 'FLIPs' are are trademarks used by Innovative Bioimaging, s.r.o.

1137

INSIHGT - Scalable, Accessible, Homogeneous Deep Multiplexed Immunolabelling Platform for 3D Spatial Biology

Dr Hei Ming Lai[1,2], Mr Jacky Tin Shing Hung[2,3], Mr Juno Chun Ngo Yau[2], Mr King Ngai Chow[2], Mr Thomas Chun Yip Wong[2]

[1]Department of Chemical Pathology, The Chinese University of Hong Kong, Shatin, New Territories,, Hong Kong SAR, China, [2]Li Ka Shing Institute of Health Sciences, The Chinese University of Hong Kong, Shatin, New Territories,, Hong Kong SAR, China, [3]Department of Psychiatry, The Chinese University of Hong Kong, Shatin, New Territories,, Hong Kong SAR, China

LS-02 (2), Lecture Theater 4, august 26, 2024, 14:00 - 15:00

Biological systems are complex, encompassing intertwined spatial, molecular and functional features. However, methodological constraints always limit the completeness of information that can be extracted. Here, we report the development of INSIHGT, a minimally perturbative and cost-efficient three-dimensional (3D) spatial biology method utilizing solvent perturbative chemistry. This allows quantitative, highly multiplexed and multi-modal readout of tissue biomolecules in up to centimeter-scale biological systems. Diverse antigens, mRNA transcripts, neurotransmitters, and post-translational and epigenetic modifications, are well-preserved and visualized, allowing multi-round molecular probing for high-dimensional spatial biology and compatibility with downstream traditional histology. With INSIHGT, we mapped previously undescribed podocyte-to-parietal epithelial cell microfilaments and demonstrated their geodesic clustering in mouse glomeruli, catalogued sparsely located neurofilament-intensive inclusion bodies in the human cerebellum, and identified NPY-proximal cell types defined by spatial morpho-proteomics in mouse hypothalamus. We anticipate INSIHGT can form the foundations for 3D spatial multi-omics technology development and holistic systems biology studies.

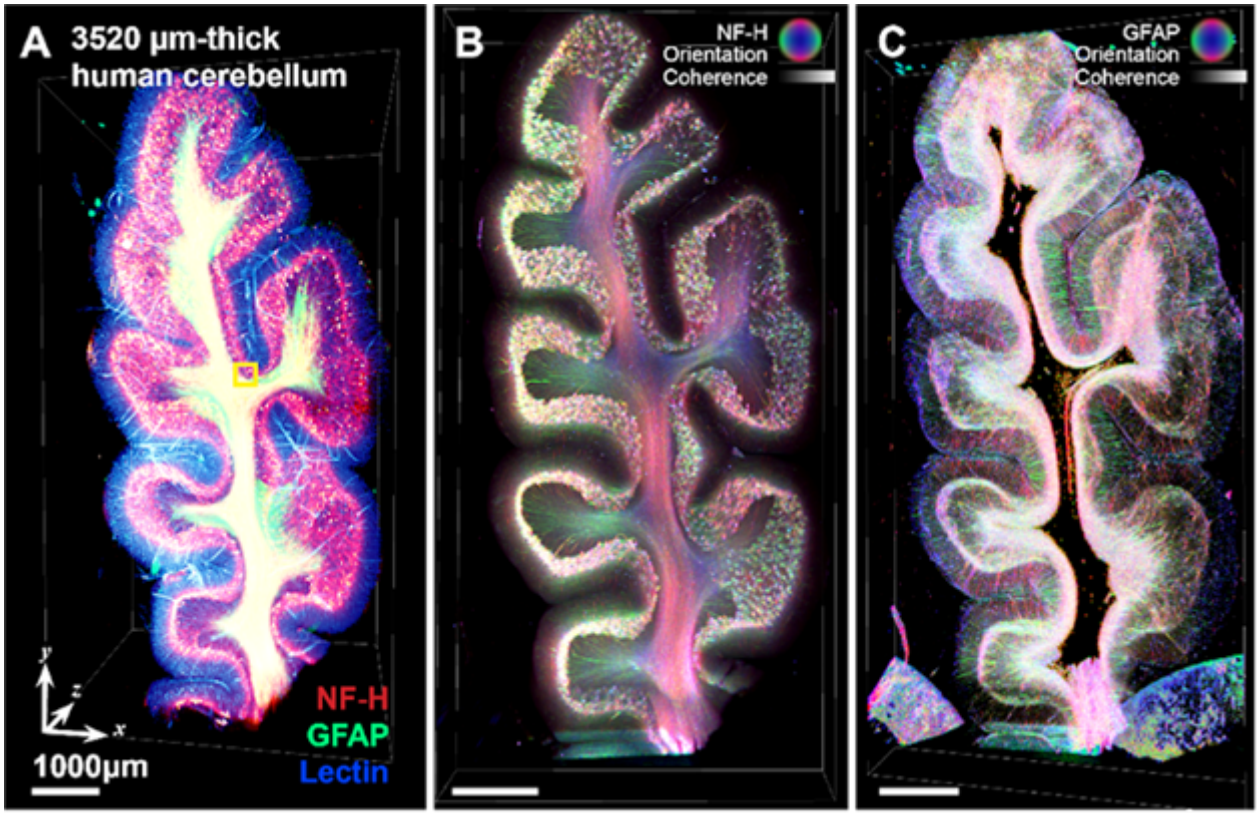

Keywords:

3D spatial biology, systems biology

Reference:

Lai et al. (2022). Antibody stabilization for thermally accelerated deep immunostaining. Nature Methods. 19, 1137–1146.
Yau et al. (2023). Principles of deep immunohistochemistry for 3D histology. 3, 100458.

24

The Best of Both Worlds: Combining Label Free and Fluorescence Imaging with Livecyte

Peter Djali[1], Dr Meetal Jotangia[1]
[1]Phase Focus Ltd, Sheffield, United Kingdom

Poster Group 1

Fluorescent imaging can reveal much about cellular function but can also be a double-edged sword with both phototoxic and cytotoxic consequences that can impair normal cell function or even induce cell death. Livecyte's label-free live-cell imaging is a powerful quantitative phase technique, generating high-contrast, fluorescence-like images using low powered illumination in which cells appear as bright objects on a dark background. The enhanced contrast increases the robustness of single-cell segmentation and tracking without the need for dyes, maintaining true physiological conditions over a long period of time. Additionally, Livecyte offers the best of both worlds: - intermittent fluorescence imaging reduces the potential detrimental effects and can be linked to the more frequent non-perturbing label-free images.

Our previous studies have reported the detrimental effects to normal cell division of the nuclear live-cell imaging stain SiR-DNA when compared with non-perturbing label free imaging on the Livecyte. The inclusion of SiR-DNA reduced both cell count and total dry mass in a LED power dose-dependent manner relative to non-illuminated and unlabelled conditions suggesting fluorescence altered cells natural growth and proliferation rate. Alongside this, SiR-DNA and illumination increased median cell area which correlated with changes in average dry mass per cell compared to controls. Being able to look at multiple parameters indicates a cell profile of phototoxicity with slowed division and accumulation of mass leading to a large, oversized phenotype.

Such effects will be even more enhanced when dealing with sensitive primary cells such as T-Cells and Neuronal cells. We now show how we can track neuronal outgrowth completely label free, by a unique combination of brightfield and Livecyte label free technique, and how an advanced T-Cell assay can be built in which the sensitive primary effector cells remain entirely label free.

T cell killing assays traditionally yield little or no information on the T to Target interactions and would rely on fluorescence labelling of photo vulnerable primary T cells. However, Livecyte can gain a plethora of T cell interaction kinetics with target cells including the time and number of T cell contacts with a target cell before cell death occurred. All of this without having to label T cells giving more meaningful insights on how your engineered T cells are behaving and more predictive information for in vivo studies.

Livecyte's label free imaging and analysis has also set a new precedence for neurite outgrowth assays. Neuronal cells are also more at risk of phototoxicity limiting our ability to image over long periods of time and to look at network formation dynamically. With Livecyte's advanced analysis recipe, neurite outgrowth can be quantified from the initial changes in cell morphology and migration as cells form attachments through to network formation and metrics such as the number of branching points and total neurite length, gaining a novel understanding of the effect of therapeutic drugs on the dynamics of neurite outgrowth.

There is mounting evidence revealing multiple off-target effects and phototoxicity caused by fluorescence excitation probes with reactive oxygen species being the predominant cause of

phototoxicity [1,2]. Livecyte versatility enables either non-invasive QPI only or with a possibility of intermittent fluorescence imaging producing a plethora of time sensitive single-cell information where there is a strong need to protect the cells. This provides invaluable data to researchers using fluorescence to investigate subtle changes in cell behaviour and phenotype.

References

1. Magidson V, Khodjakov A (2013). Circumventing photodamage in live-cell microscopy. Methods Cell Biol. 114:545-60.
2. Douthwright S, Sluder G 2017. Live Cell Imaging: Assessing the Phototoxicity of 488 and 546 nm Light and Methods to Alleviate it. J Cell Physiol 232(9):2461-2468

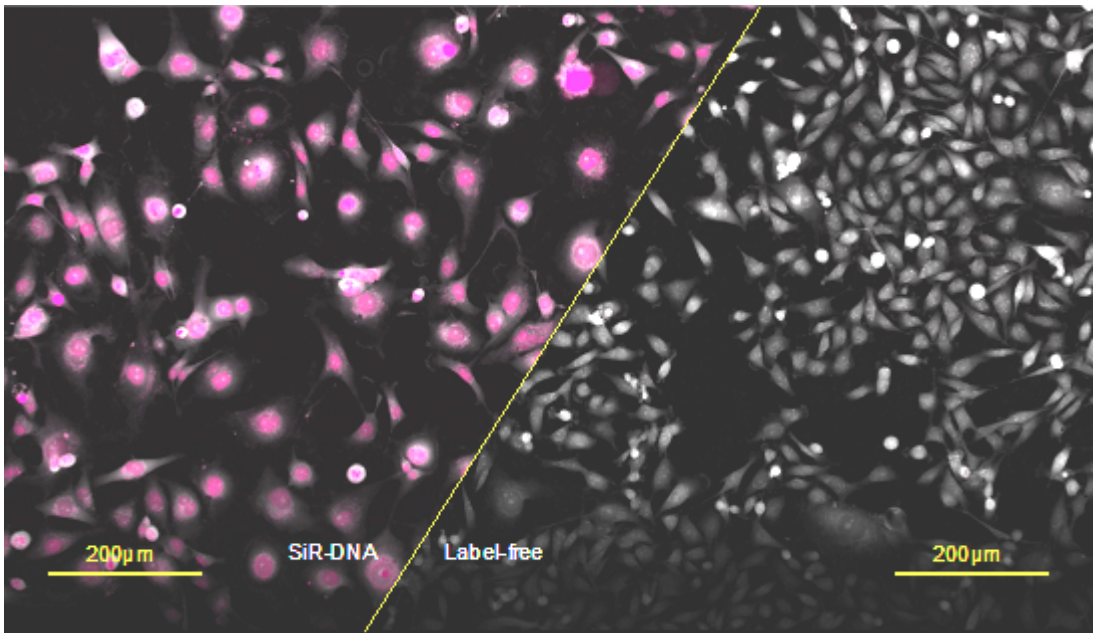

Keywords:

live-cell label-free, QPI, Killing-Assay, Neurite-Outgrowth

207

Paleopalynology of Holocene birch hybridization in Iceland

Kesara Anamthawat-Jonsson[1]
[1]Institute of Life and Environmental Sciences, University of Iceland, Reykjavik, Iceland

Poster Group 1

Betula L. (birch) is a genus of about 50–60 tree species distributed throughout the temperate, boreal, and arctic regions of the Northern Hemisphere. Birch woodlands are an integral component of the tundra biome, and birch is one of the key broad-leaved tree species of the circumpolar boreal forest. Birch woodlands in Iceland, which cover around 1.5% of the total land area, are composed of 80% birch shrubs less than 2 m tall. Similar birch shrubs, often referred to as mountain birch, are found in Fennoscandia, northern Russia, European mountain regions and beyond. Previous botanical, cytogenetic and molecular genetic studies have shown that shrub-like birch in Iceland is the result of introgressive hybridization between the two co-existing Betula species, the arctic dwarf birch (Betula nana) and the European downy birch (B. pubescens). As dwarf birch is a diploid species and downy tree birch a tetraploid species, their hybrids are triploid. In the introgression process, triploid hybrids, which are partially fertile, can backcross with the parental species, producing progenies comprising introgressed diploid, triploid, and tetraploid plants. Triploid plants produce both normal triporate pollen (with three pores) and abnormal, aborted pollen, due to dysfunctional meiosis. The type of pollen abnormality that can be detected and quantified is non-triporate pollen (with four or more pores in the pollen wall). The presence of non-triporate pollen was therefore used in the study resented here as a marker to trace birch hybridization in the past. In this study fossil pollen in samples from peat sediments was examined. The peat monoliths were extracted from three geographically diverse locations in Iceland, from Grímsnes (S), Eyjafjördur (N) and Thistilsfjördur (NE Iceland), and throughout the Holocene epoch. Ages were calibrated based on known volcanic tephra layers and by radiocarbon dating. By measuring the size of individual pollen grains, we were able to differentiate pollen of the shrub-like downy birch (B. pubescens) from its closely related dwarf birch species (B. nana). The results revealed an establishment and a rapid expansion of birch woodland predominated by shrub birch B. pubescens soon after the retreat of the Icelandic Pleistocene icesheet. Non-triporate pollen grains were detected in samples from all three locations and throughout the Holocene, but with different frequencies. The results showed peaks of intense hybridization following woodland expansion in the initial period of the Holocene, from about nine thousand years ago, and again in the warming period of the mid-Holocene Thermal Maximum, the period between five and three thousand years ago. Triploid hybrids that were produced during the intense period of hybridization could potentially backcross with the dwarf birch or the downy birch, allowing gene flow by introgression between the two species, presumably making birch more adaptive to environmental changes. Thus, climate warming in the current era is expected to promote this introgressive hybridization resulting in a significant change of landscape of the birch woodland in Iceland. Birch woodlands are likely to become more widespread. Furthermore, introgressed shrub birch is likely to be more competitive over dwarf birch as average summer temperature rises.
Acknowledgements: I would like to thank Lilja Karlsdóttir and Ægir Thór Thórsson for their collaborative work combining paleopalynology with botanical, cytogenetic and molecular genetic analyses of woodland birch in Iceland.

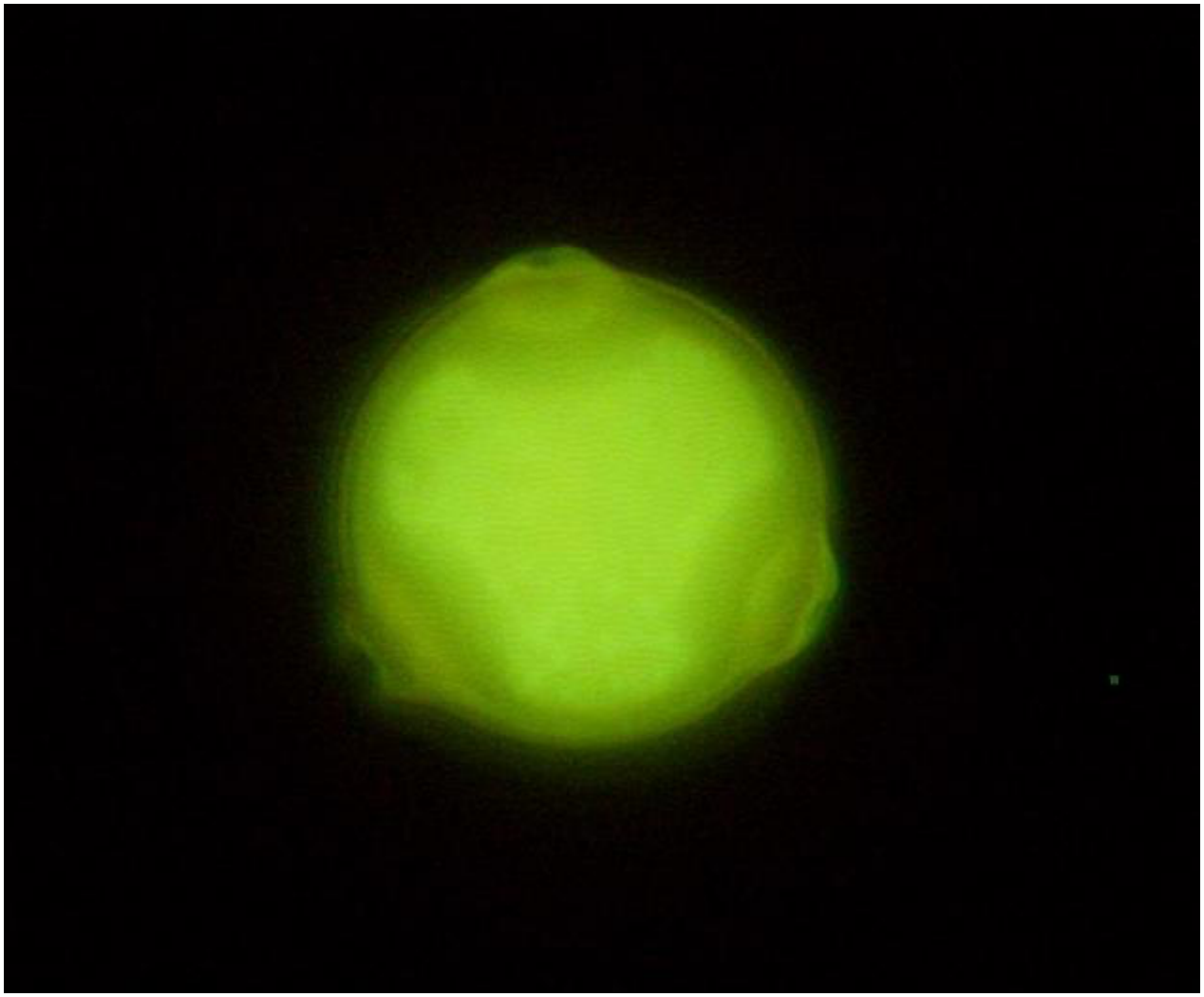

Keywords:

Betula, birch, palynology, pollen, triploids

Reference:

1. Anamthawat-Jónsson K, Karlsdóttir L, et al. (2023) J Microscopy 291: 128-141.
2. Anamthawat-Jónsson K, Karlsdóttir L, et al. (2021) New Forests 52: 659-678.
3. Anamthawat-Jónsson K (2019) Science Asia 45: 203-211.
4. Karlsdóttir L, Hallsdóttir M, et al. (2012) Rev Palaeobot Palyn 181: 1-10.
5. Thórsson ÆTh, Pálsson S, et al. (2010) J Biogeogr 37: 2098-2110.

310

Exploring the 3D architecture of native and stained human intervertebral discs through micro-CT

Raluca-Ana-Maria Barna[1,3,4], Federica Orellana[1,2], Marie-Rosa Fasser[4,5], Daniel Valent[4], Jonas Widmer[4,5], Annapaola Parrilli[1]
[1]Empa - Center for X-Ray Analytics, Dübendorf, Switzerland, [2]University of Fribourg, Fribourg, Switzerland , [3]University of Bern, , Switzerland, [4]Balgrist University Hospital - Spine Biomechanics, Zurich, Switzerland, [5]Balgrist University Hospital - Department of Orthopedics, Zurich, Switzerland

Poster Group 1

Background incl. aims
The disruption of normal intervertebral disk (IVD) structure and its subsequent degeneration significantly contributes to the onset of low back pain [1]. To date, the human IVD 3D microstructure characterization has been confined to imaging the annulus fibrosus (AF) [2] and the subchondral endplate [3]. Our study aimed to propose a step-wise approach for the complete morphological investigation of human IVDs at various tissue processing stages using a non-destructive micro-CT analysis. This approach allowed detailed 3D visualization of distinct IVD anatomical components: nucleus pulposus (NP), AF, and the orientation of collagen fibers. Additionally, the method provided a precise quantification of lesions and calcifications within the disk, which affect the integrity of its microstructure and thus its functional and biomechanical characteristics [4].

Methods
The IVDs (n = 14) were examined through the use of the micro-CT EasyTom XL Ultra 230–160 micro/nano-CT scanner (RX Solutions, Chavanod, France) with a voxel size of 40 µm. Each sample was scanned label-free (both frozen and thawed) and after formalin fixation and staining of the tissue in an iodine-based contrast agent solution. The calcifications and lesions present in the tissue were determined with an automatic segmentation approach using the software Avizo (Thermo Fisher Scientific, MA, USA). For each processing stage, the calcification and lesion volume fractions were compared considering the entire disc and selecting the AF region. In addition, the degree of contrast enhancement has been defined calculating the Hounsfield Units (HU) relative to the acquired CT values.

Results
Thawed samples allowed an accurate quantitative analysis of lesions and calcifications present in the native IVD. Additionally, the analysis of frozen samples provided valuable insight into the alternate laminal pattern of the AF. Iodine staining, while providing a homogeneous increase in contrast and simultaneous visualization of the IVD anatomical components, was time-consuming (2 weeks of staining) and resulted in the extrusion of the NP, leading to an increase in lesion volume fraction. The contrast measured in HU increased between the different preparation steps.

Conclusion
The examination of frozen, thawed, and chemically fixed-stained IVD tissues using micro-CT revealed distinctive microstructural information, presenting different benefits for each stage. The systematic methodology used in this study had the aim to define the trade-off between contrast enhancement and processing artefacts. A label free imaging of the IVD represents a valuable option for a 3D morphological investigation of the sample, especially when combined with biomechanical testing due to its non-destructiveness thus preserving the original stiffness and geometry.

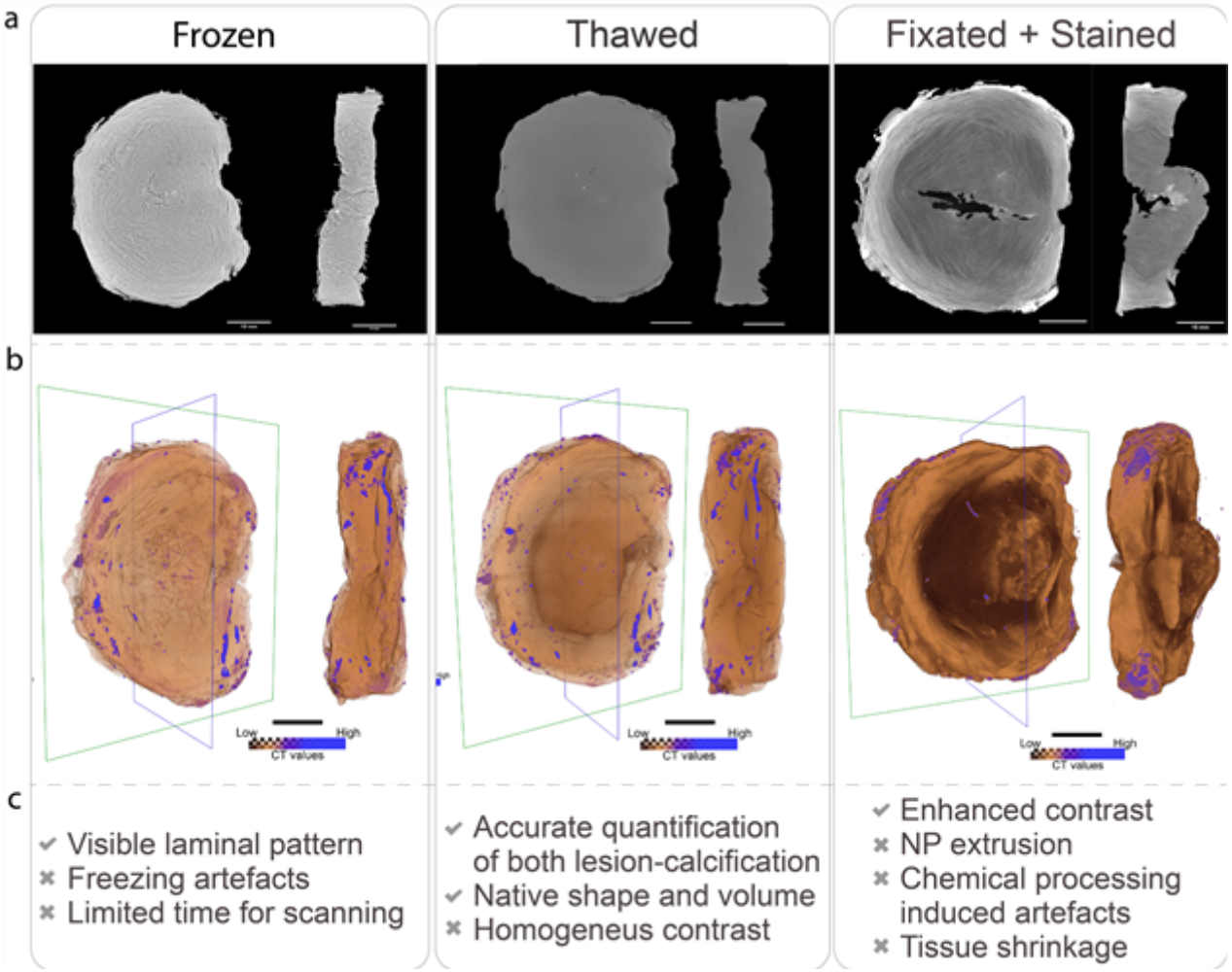

Keywords:

Micro-CT, IVD, 3D-anatomy, X-ray imaging

Reference:

[1] Diwan A D, Melrose J (2022) Intervertebral disc degeneration and how it leads to low back pain. JOR Spine 6(1):1-23.
[2] Stein D, et al. (2021) 3D virtual reconstruction and quantitative assessment of the human intervertebral disc's annulus fibrosus: a DTI tractography study. Sci Rep 11:6815.
[3] Rutges J P, et al. (2011) Micro-CT quantification of subchondral endplate changes in intervertebral disc degeneration. Osteoarthritis Cartilage 19(1):89-95.
[4] Whatley B R, Wen X (2012) Intervertebral disc (IVD): Structure, degeneration, repair and regeneration, Materials Science and Engineering: 32(2):61-77.

357

The effect of mesenchymal stem cell's secretome on hyperglycemia-related complications: focus on reproductive system disorders

Dr. Basak Isildar[1]
[1]Balikesir University Faculty of Medicine Histology and Embryology Department, Balıkesir, Türkiye

Poster Group 1

Background incl. aims
Type 1 diabetes (T1D) is characterized by insulin deficiency due to the autoimmune destruction of β-cells in the pancreas, which causes hyperglycemia. Although exogenous insulin is very effective in increasing the survival of patients, inadequately controlled hyperglycemia leads to secondary complications. One of the complications associated with T1D is reproductive disorders. In males with long-standing T1D, this can appear as sexual dysfunction or reproductive issues, primarily stemming from impaired spermatogenesis, reduced testosterone production and release, and changes in glucose metabolism within Sertoli cells [1]. Mesenchymal stem cells (MSCs) hold promise for handling the therapeutic requirements of T1D due to their involvement in the immunomodulation process and cytoprotective, antiapoptotic, and antioxidant properties. It is established that MSCs exert their therapeutic effects via paracrine mechanisms, releasing a diverse array of bioactive molecules termed the secretome, which includes growth factors, cytokines, chemokines, exosomes, and other bioactive factors. The composition of the secretome can be modified through various inductions, presenting significant potential for targeted therapy development. Among these induction types are a hypoxic cell culture environment, cultivating the cells on a three-dimensional scaffold, and using various chemicals. Conditioned media (CM) represents a tool to use the therapeutic benefits of the secretome exclusively, obtained by collecting the medium in which MSCs are cultured, free of cellular components [2]. The CM is important in the treatment of T1D due to the factors it contains [3]. Furthermore, the systemic application of CM could be crucial in preventing and repairing tissue damage caused by hyperglycemia in the body, despite this not being the primary treatment goal. This comprehensive approach is valuable as it addresses the entirety of T1D, which affects the entire organism. So, this study aims to investigate the effects of human umbilical cord MSC-derived CM, used for therapeutic purposes in the rat experimental T1D model, on testicular damage and the disrupted hormone mechanism, caused by hyperglycemia.
Methods
MSCs were isolated from human umbilical cord tissue by the tissue explant method, followed by characterization experiments. Two distinct CM types were obtained: CM obtained from MSCs cultured in normal culture (N-CM) conditions and CM obtained from MSCs preconditioned with a hypoxia mimetic agent, deferoxamine (150 µM) (DFX-CM). Sprague-Dawley rats were used for in vivo experiments, and the T1D model was induced using a single high-dose of streptozotocin (55 mg/kg). Experimental groups included control (C), diabetes (D), diabetes with N-CM treatment (D+N-CM), and diabetes with DFX-CM treatment (D+DFX-CM), with 6 rats in each group. Following the 4th week of the STZ injection, diabetic rats received intraperitoneal injections of equal amounts of N-CM and DFX-CM (each containing at least 15 µg of protein) four times a week for three weeks. Blood samples for hormone analysis were collected via cardiac puncture one week after the final CM dose injection, and the rats were sacrificed. After sacrification, serum levels of gonadotropin-releasing hormone (GnRH), follicle-stimulating hormone (FSH), luteinizing hormone (LH), and testosterone were quantified via enzyme-linked immunosorbent assay (ELISA) for hormonal profiling. Testicular tissues stained with hematoxylin and eosin were used to perform Johnsen's scoring via light microscopy to assess spermatogenesis. For this analysis, an average of 10 seminiferous tubule sections were analyzed in each rat (n=3). Seminiferous tubule diameter and epithelial thickness were also measured

using the Image J analysis program. Finally, cellular ultrastructure was examined using transmission electron microscopy (TEM). All findings are presented as preliminary outcomes. Statistical analysis was conducted using the Kruskal-Wallis test, with p-values <0.05 considered significant.

Results

Upon examination of reproductive hormone levels in serum, statistical significance was identified among the groups for GnRH, FSH, and LH ($p<0.05$, $p<0.001$, and $p<0.05$, respectively). All hormone levels decreased in the D group. It was noteworthy that GnRH, FSH, and testosterone levels tended to increase in the D-DFX-CM group compared to the D group. Johnsen's scoring indicated impairment in spermatogenesis in the diabetes groups. On the other hand, the measurements of seminiferous tubule diameter and epithelial thickness did not reveal statistically significant differences. TEM analysis of seminiferous tubules revealed that the C group exhibited normal morphology. In contrast, the D group exhibited elevated lysosome levels in Sertoli cells, spermatogonia with dispersed heterochromatin, and primary spermatocytes with disintegrated nuclear membranes, alongside increased intercellular spaces. In both treatment groups, such defects were relatively less than in the diabetic group, and a substantial improvement in the ultrastructure of Sertoli and spermatogenic cells within the seminiferous epithelium was observed. Examination of spermatids showed that some in the diabetes group had impaired chromatin condensation. Axoneme structures were generally preserved (Fig.1).

Conclusion

Ultrastructural examinations revealed that the secretome of MSCs improved the seminiferous tubule epithelium by exerting a cytoprotective effect. Despite no significant impact on the hypothalamic-pituitary-gonadal axis, which is impaired by hyperglycemia, it is noteworthy that DFX-CM increased GnRH and testosterone release from the hypothalamus. However, this effect was insufficient, leading to no observable improvement in spermatogenesis. These preliminary findings underscore the necessity for further investigation into the observed ultrastructural improvement in the seminiferous epithelium and the need to uncover new cellular-level data elucidating the mechanisms of action of the secretome of MSCs.

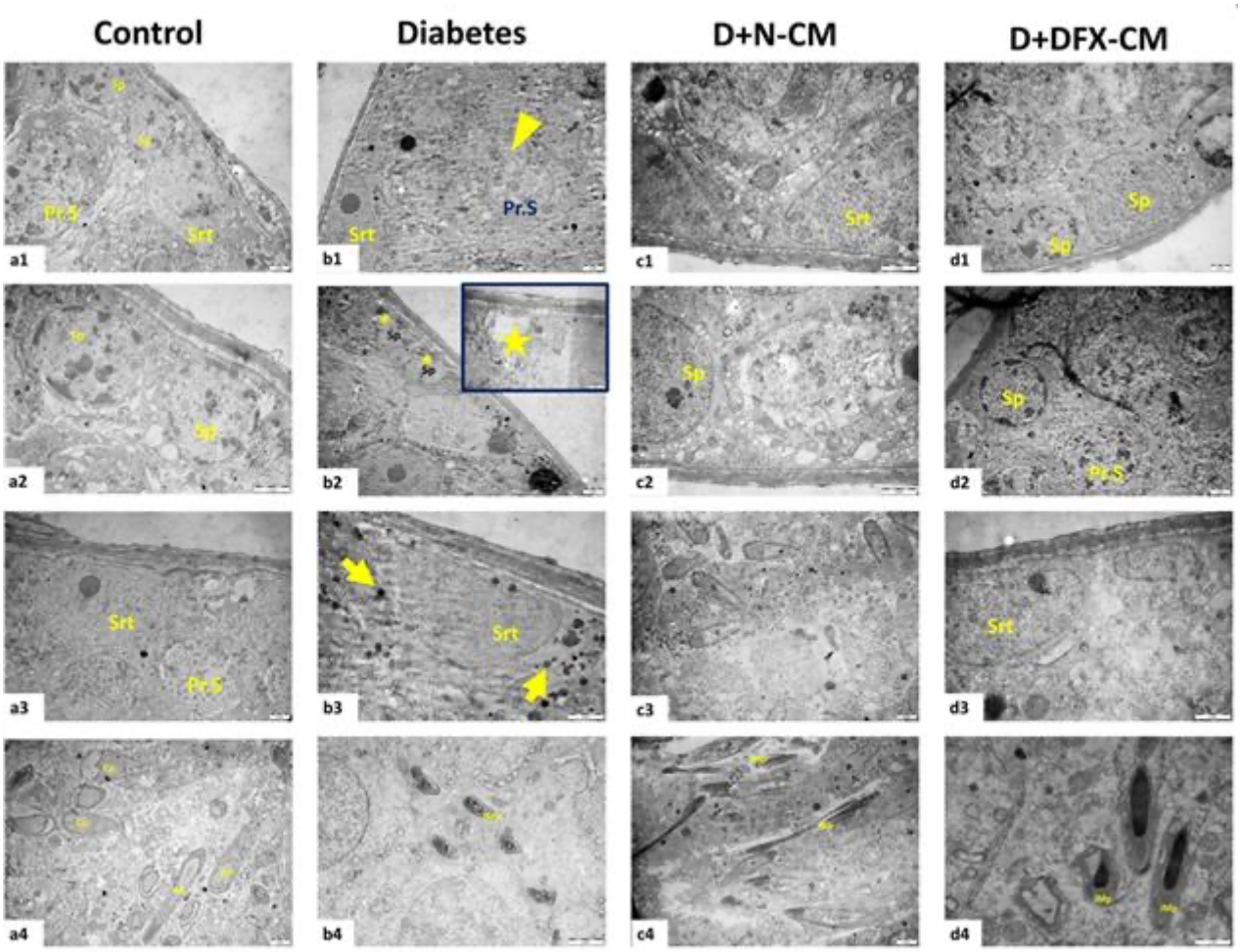

Representative figures of transmission electron microscopic evaluations for control (**a**), diabetes (**b**), D+N-CM (**c**) and D+DFX-CM (**d**) groups. **Sp**: Spermatogonium, **Pr.S**: Primary spermatocytes, **Srt**: Sertoli cells, **Cp**: Cap phase, **Ap**: Acrosomal phase, **iMp**: initial maturation phase, **Mp**: maturation phase, **arrow**: lysosome, **star**: intercellular space, **asterisk**: dispersed heterochromatin of Sp and **arrow head**: disintegrated nuclear membrane

Keywords:

Mesenchymal stem cells-Testicular damage-Conditioned medium

Reference:

1. Baghel K, Azam Z, Srivastava R, Gupta N, Kango N. Withaferin-A attenuates diabetes mellitus induced male reproductive dysfunction mediated by ERα in brain and testes of Swiss albino mice. Sci Rep [Internet]. 2023;13(1):1–23. Available from: https://doi.org/10.1038/s41598-023-44904-y
2. Su Y, Xu C, Cheng W, Zhao Y, Sui L, Zhao Y. Pretreated Mesenchymal Stem Cells and Their Secretome: Enhanced Immunotherapeutic Strategies. Int J Mol Sci. 2023;24(2).
3. Isildar B, Ozkan S, Koyuturk M. Therapeutic Potential of Mesenchymal Stem Cell-Derived Conditioned Medium for Diabetes Mellitus and Related Complications. Adv Ther. 2023;2300216.

745

A new protocol for fluorescent quantitative labeling of individual proteins for live cell internalization assays

Dr Juan De Dios Alche[1,3], Dr. Alfonso Clemente[2], Dr. Antonio J. Castro[1]
[1]Department of Stress, Development and Signaling in Plants. Estacion Experimental del Zaidin. CSIC, Granada, Spain, [2]Department of Nutrition, Gastrointestinal Health and Food Safety. Estacion Experimental del Zaidin. CSIC, Granada, Spain, [3]University Institute of Research on Olive Grove and Olive Oils, Jaen, Spain

Poster Group 1

Background
A single protein can be chemically labeled with different fluorescent dyes in order to get insights about its cellular localization and molecular mechanism of action [1]. Overall, an ideal fluorescent dye should be specific and stable, and should not interfere with the physicochemical and conformational properties of the protein. For internalization assays in living cells, organic fluorophores such as fluorescein (FITC) and rhodamine (TRITC) are the dyes of choice since they have a short lifetime (<5 ns), and they are brighter and more photostable than other fluorescent labels [2]. They also have a small size, thus interfering less with the biological system (i.e. protein). The main disadvantages of these compounds are their low specificity and unknown binding stoichiometry. In this work, we have tailored a minimal labeling protocol, originally developed for proteomic applications, in order to tag single proteins for being used in live cell internalization assays.

Methods
The original 2D-DIGE minimal labeling protocol ensures that only 1–2% of the available Lys is labeled. Thus, this protocol facilitates successful labeling of an individual protein at a specific location (ε amino group of Lys) and with a well-defined stoichiometry (1:1). Moreover, this modification only adds just about 500 Da to the protein total molecular weight, thus minimizing perturbations of the physicochemical and conformational properties of the protein. Overall, the full standard protocol is accomplished in 4-5 hours and comprises three different steps (Figure 1). Firstly, the protein of interest is resuspended in the reconstitution buffer and labeled with the CyDye fluorophore of choice. After incubation, labeling is stopped by adding an excess of L-lysine (Lys) to the reaction mixture. Secondly, the excess of free Lys-bound CyDye is removed to minimize background in the internalization experiments. At this point, the Cy-labeled protein can be concentrated if necessary, by filtration through a size exclusion membrane of suitable cutoff. Finally, in the last step, the quality of the labeling reaction is tested by SDS-PAGE.

Results
To validate experimentally our protocol, we carried out the fluorescent labeling of IBB1, a major soybean protease isoinhibitor of the Bowman-Birk family that is currently being investigated as colorectal chemopreventive agent [3], with two different CyDye fluors. A single protein band of about 12 kDa was visible after scanning the polyacrylamide gel at 488 nm (IBB1-Cy2) or 635 nm (IBB1-Cy5), respectively, proving the success of the minimal labeling reaction. Then, we monitored the in vivo internalization dynamics of the labeled IBB1 protein in human colorectal adenocarcinoma HT29 cells. We observed that the CyDye-labeled IBB1 proteins crossed the plasma membrane of HT29 cells after a few minutes and was gradually accumulated, forming fluorescent patches randomly distributed across the cytoplasm. We also tested the suitability of this method for carrying out multiplex experiments. Thus, two different combinations of labels were tested. Firstly, IBB1-Cy2 internalization was combined with nuclei staining using Hoechst 33342 dye. The fluorescent signal of IBB1 did not

overlap with Hoechst-specific labeling, indicating that the protein did not internalize into the cell nucleus. Secondly, IBB1-Cy2 internalization was combined with the fluorescent probe FM 4-64, an endocytic tracer [4]. We observed that the fluorescent signal from the endosome marker colocalized with the Cy2-labeled IBB1 protein in the cytoplasm of HT29 cells, suggesting that IBB1 is internalized through one of the existing endocytosis pathways.

Conclusions

In this work, we have adapted a protocol that was originally developed for two-dimensional fluorescence difference gel electrophoresis (2D-DIGE) applications, to label proteins with CyDye fluors for single-molecule internalization assays in living cells. This protocol is suitable for both proteins purified from their natural sources and recombinant proteins expressed in heterologous systems (e.g. E. coli, P. pastoris, etc.). This “minimal labeling” method offers a number of advantages including specificity and known stoichiometry, simplicity, high reproducibility, and sensitivity and allows multiplexing while minimizing perturbations of the biological system. Moreover, the minimal labeling protocol is suitable for multiplex experiments, either combining up to three different proteins labeled with Cy2, Cy3, and Cy5, respectively, or using CyDye fluors together with other fluorescent labels. Finally, since only a single lysine (Lys) residue per protein molecule is labeled, this method is also quantitative.

This research was funded by projects AGL2017-84298-P and AGL2017-83772-R from MINECO/AEI, and PID2020-113324GB-100 and TED2021-130015B-C22 from MICIIN/AEI, all of them cofinanced by the ERDF program of the European Union.

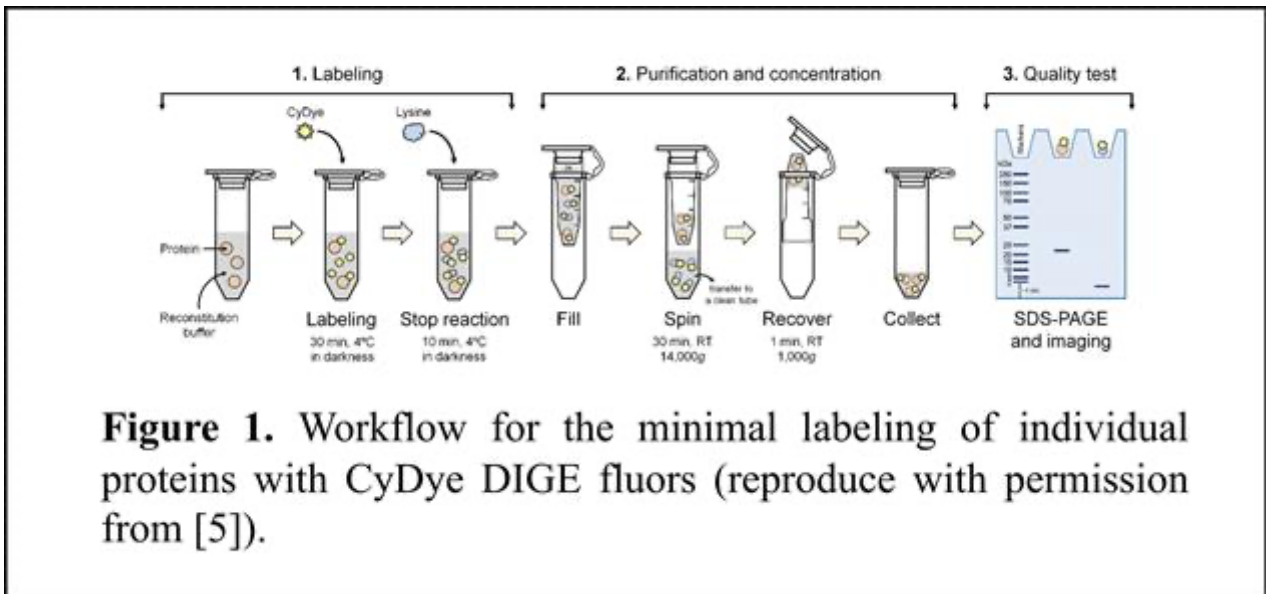

Figure 1. Workflow for the minimal labeling of individual proteins with CyDye DIGE fluors (reproduce with permission from [5]).

Keywords:

CyDye-fluors, IBB1, internalization-assays, minimal fluorescent-labeling

Reference:

[1] Toseland CP (2013) Fluorescent labeling and modification of proteins. J. Chem. Biol. 6: 85-95.
[2] Ha T, Tinnefeld P (2012) Photophysics of fluorescent probes for single-molecule biophysics and super-resolution imaging. Ann. Rev. Phys. Chem. 63: 595-617.

[3] Clemente A, Marín-Manzano MC, Jiménez E, Arques MC, Domoney C. (2012) The anti-proliferative effects of TI1B, a major Bowman-Birk isoinhibitor from pea (Pisum sativum L.), on HT29 colon cancer cells are mediated through protease inhibition. Br. J. Nutr. 108: S135-S144.
[4] Bolte S, Talbot C, Boutte Y, Catrice C, Read ND, Satiat- Jeunemaitre B. (2004) FM-dyes as experimental probes for dissecting vesicle trafficking in living plant cells. J. Microsc. 214: 159-173.
[5] Castro AJ, Clemente A, Alché JD (2020) A protocol for minimal single protein labeling with CyDye fluors for live cell internalization assays. In: Fluorescent methods for investigation of living cells and microorganisms, Grigoryeva N. (Ed.). IntechOpen, London, UK. pp. 1-14.

778

Exploring Cell-Material Interactions at Focal Adhesion Points

Dr Krzysztof Berniak[1], Dr Daniel P. Ura[1], Prof. Adam Piórkowski[2], Prof. Urszula Stachewicz[1]
[1]Faculty of Metals Engineering and Industrial Computer Science, AGH University of Krakow, Kraków, Polska, [2]Department of Biocybernetics and Biomedical Engineering, AGH University of Krakow, Kraków, Polska

Poster Group 1

Background
In tissue engineering, electrospun fibers are pivotal scaffolds, shaping cell interactions through their mechanical strength and surface characteristics. Focal adhesion sites, multi-protein complexes, regulating cell adhesion dynamics, form mechanical links between intracellular actin bundles and the substrate. Widely used in bioengineering, PMMA fibers play a crucial role as an integral component of bone implants, serving as an adhesive platform for various cell types (1). The aim of the research is to investigate the distribution and structure of proteins paxillin and vinculin in focal adhesion (FA) sites using advanced microscopy techniques, particularly AiryScan confocal super-resolution microscopy and the Density-Based Spatial Clustering of Applications with Noise (DBSCAN) cluster algorithm. Moreover, this research is performed on cells bind to polymer fibers commonly used in tissue scaffolds and compared to standard glass slides. Therefore, our results contribute to designing scaffold and understanding the interactions between cells and materials applied in/for tissue regeneration.
Methods
PMMA fibers were electrospuned using the EC-DIG apparatus with climate control. Studies involved human osteoblast-like cell line MG-63 on PMMA electrospun fibers. Cells were cultured under standard conditions, fixed, and permeabilized after 3 days. Actin filaments were visualized with Alexa Fluor 488 Phalloidin, and nuclear DNA was stained with DAPI. Focal adhesion proteins (vinculin and paxillin) were labeled with immunofluorescence. Confocal microscopy, specifically Zeiss LSM 900 with the high-resolution concept Airyscan, captured multicolor 3D microscopy images of cells connecting to PMMA fibers. Image analysis was performed by using ImageJ.
Results
AiryScan microscopy offered detailed insight into cell adhesion onto PMMA fibers, confirming the binding process. Additionally, DBSCAN cluster analysis revealed substrate-specific correlations in osteoblast behavior, providing a quantitative understanding of cell-PMMA interactions. Effective adhesion correlated with well-organized, larger focal adhesions characterized by increased protein accumulation. Interestingly, a shift in paxillin and vinculin signals was observed during cell attachment to both glass and polymer fibers. Focal adhesions on polymer fibers appeared smaller and elliptical but exhibited higher protein density compared to glass (2). These attributes, influenced by paxillin and vinculin, likely signify cell adhesion strength. This innovative cluster analysis uncovers variations in adhesion clusters, offering valuable insights for scaffold design refinement, diverse substrate adhesion evaluation, and enhanced cellular interactions in biomedical applications.
Conclusion
We introduce a new method for analyzing protein distribution in cell adhesion to polymer fibers, crucial for tissue engineering scaffolds. Our study reveals significant differences in adhesion complex distribution compared to glass, with a focus on vinculin and paxillin. By quantitatively comparing osteoblast adhesion on glass and polymer scaffolds, we provide the first detailed analysis in a model incorporating polymer fibers, paving the way for understanding cell-material interactions in medical biomaterial research.

Acknowledgements
This study was conducted within “Nanofiber-based sponges for atopic skin treatment” project carried out within the First Team program of the Foundation for Polish Science co-financed by the European Union under the European Regional Development Fund, project no POIR.04.04.00-00- 4571/17-00 and BioCom4SavEn project funded by the European Research Council under the European Union's Horizon 2020 Framework Programme for Research and Innovation (ERC grant agreement no. 948840)

Keywords:

adhesion, fibers, PMMA, paxillin, Airyscan

Reference:

(1) Ura, D. P.; Karbowniczek, J. E.; Szewczyk, P. K.; Metwally, S.; Kopyściański, M.; Stachewicz, U. Cell Integration with Electrospun PMMA Nanofibers , Microfibers , Ribbons , and Films : A Microscopy Study. Bioengineering (Basel) 2019, 6 (41), 41. https://doi.org/10.3390/bioengineering6020041.
(2) Berniak, K.; Ura, D. P.; Piórkowski, A.; Stachewicz, U. Cell-Material Interplay in Focal Adhesion Points. ACS Appl Mater Interfaces 2024. https://doi.org/10.1021/acsami.3c19035

783

Self-assembly of amphiphilic dendrimers investigated by standard, cryo and liquid TEM

Dr Tom ROUSSEL[1], Pr Ling PENG[1], Pr Suzanne GIORGIO[1]
[1]CINAM - CNRS- Aix Marseille University, Marseille, France

Poster Group 1

The self-assembly of amphiphilic molecules represents a captivating avenue for the creation of innovative materials in drug delivery. In our investigation, we explore the assembling properties of amphiphilic poly(amidoamine) dendrimers, focusing on two distinct dendrimers: one terminated with tertiary amine groups N(CH3)2 denoted as dendrimer A, and another terminated with primary amine groups NH2 denoted as dendrimer B. Our study highlight the influence of surface chemical modifications on their size and packing dynamics, unveiling pathways towards finely tuned molecular architectures.
Complementary techniques of standard, Cryo and Liquid TEM are used to characterize the molecular assemblies.
Concerning dendrimer A, all the TEM technics are consistent with the formation of small nanomicelles ranging in size from 15 to 25 nm, as depicted in figures 1a and b. However, liquid TEM provides additional insights into the arrangement of dendrimers within these micelles. In the expanded view of a single micelle (fig. 1c), regularly spaced dark spots inside the micelle can be observed. The average distance between them is about 5 nm, which is comparable to the diameter of the volume containing the hydrophilic heads with tertiary amines. This supplementary information enriches our knowledge of the intricate assembly of dendrimer A within the micellar structure.
On the other hand, as seen in figures 2a and b, dendrimers B terminated with primary amine assemble in larger particles around 100 nm. Details on the assembly is clearly seen in the liquid TEM images (fig. 2b,c). The magnified image of a particle in fig. 2c corresponds to the aggregation of several micelles with size around (15- 25 nm) into a large particle of around 100 nm.
The Israelachvili assembly model's prediction1 aligns closely with the behavior of dendrimer A, illustrating its propensity to assemble into nanomicelle. However, the assembly process for dendrimer B unfolds uniquely, showcasing distinctions that necessitate a closer examination only made possible through liquid TEM. This sophisticated imaging technique unveils intricate structural nuances that had remained elusive until now, marking a significant advancement in our understanding of dendrimer assembly.
Conclusion : Our study reveals that dendrimer A exhibits consistent formation of small nanomicelles (fig. 3a) of around 20 nm, supported by various TEM techniques. Meanwhile, dendrimer B displays distinct assembly behavior (fig. 3b), forming larger particles around 100 nm. The intricate details of dendrimer A's micelle and the distinctive assembly process of dendrimer B emphasize the critical role of advanced imaging techniques such as liquid TEM in unraveling complex structural properties. This advancement significantly contributes to our comprehension of dendrimer assembly dynamics.

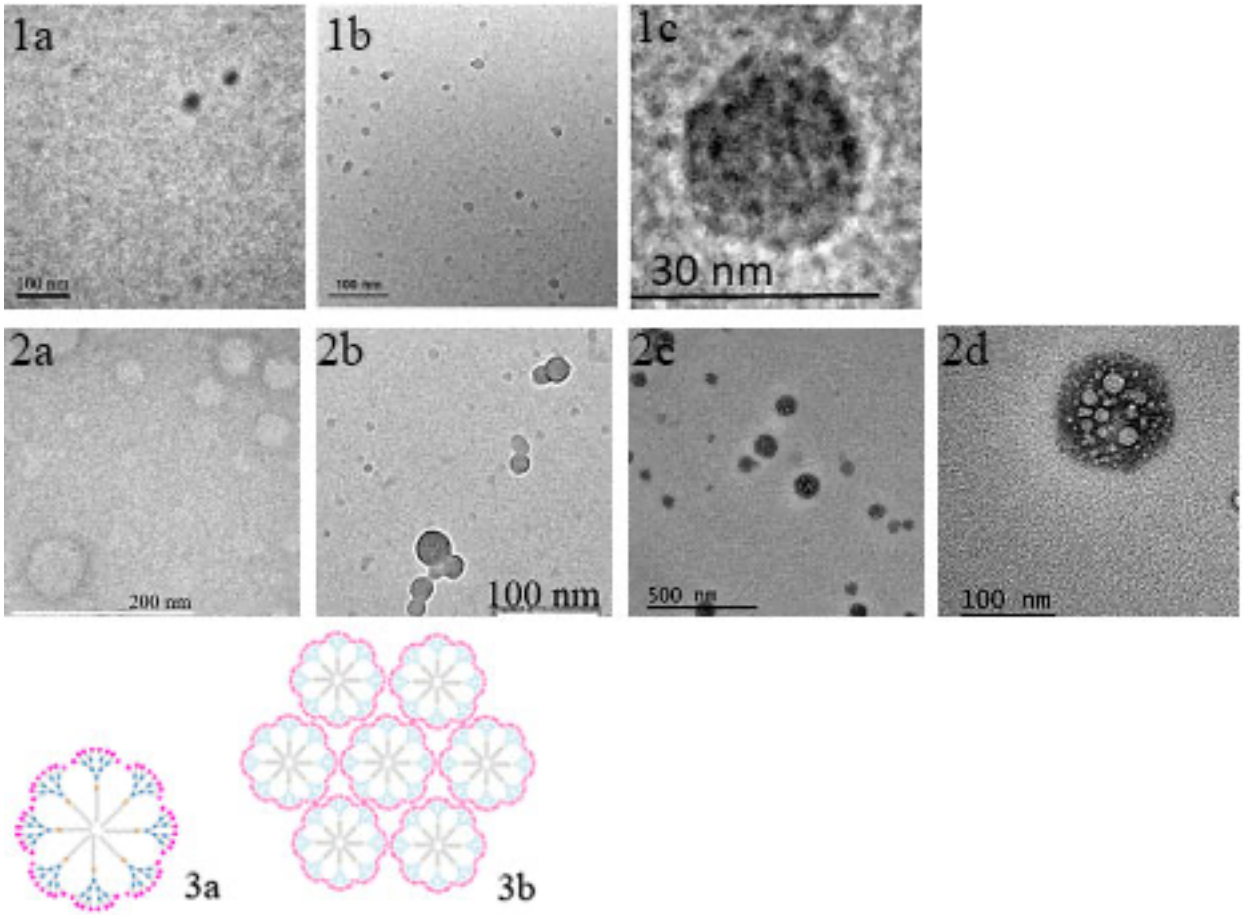

Keywords:

Nanomicelles- Cryo TEM- Liquid TEM

Reference:

1. Israelachvili, J. N., Mitchell, D. J. & Ninham, B. W. Theory of self-assembly of hydrocarbon amphiphiles into micelles and bilayers. J Chem Soc Faraday Trans 2 72, 1525 (1976).

813

Fast nanoparticle passage over cell membrane identified using 3D STED cross-sectional imaging

Dr. Boštjan Kokot[1], Hana Kokot[1], Janez Štrancar[1]
[1]J. Stefan Institute, Ljubljana, Slovenia

Poster Group 1

Background
Inorganic nanosized particulate matter (nanoparticles - NPs, a.k.a. ultrafine particles) has for a long time been known to be harmful to the environment, which is supported by recent studies.[1] What raises even more concern is the inherent toxicity of many nanoparticles once they are taken up into the body via inhalation, digestion or skin abrasion,[1] from where they translocate and affect crucial organs, such as the heart, liver and even brain.[2] Air-borne nanoparticles are especially problematic, because their inhalation is difficult to avoid and because the lungs are a very thin barrier that can easily be damaged.

Currently, some of the most recognized ways of NP entry into cells are various forms of endocytosis, e.g. phagocytosis or pinocytosis that occur in several seconds to minutes. The option of direct nanoparticle entry into the cell via physical disruption of the plasma membrane is usually not considered, although simulations confirm this is possible.[3]

In the presented work, we have exposed living murine lung epithelial cells to titanium dioxide nanoparticles and employed 3D Stimulated Emission Depletion (3D-STED) microscopy to confirm that nanoparticles can pass the plasma membrane in less than a second, suggesting a faster mode of nanoparticle entry into the cell.

Methods
The presented measurements were performed using a custom-built laser scanning Abberior STED microscope with an UPLSAPO60XW 60x water immersion 1.2 NA objective. We recorded successive xz images at 30 nm lateral pixel size and 33 nm axial pixel size, the field of 7 µm and a 30 µs dwell time per pixel. The duration of the acquired time-lapse was 50 s with a time step of 1 s. For two-color fluorescent imaging, we used a 561 nm and 640 nm laser (both having 6 µW in sample plane) in combination with a 605/50 nm and 685/70 nm filter set, respectively. To increase the lateral and axial resolution, a 775 nm STED laser with a 3D STED mask was used at 46 mW.

LA-4 lung murine cells were seeded into an Ibidi µ-dish at confluency 30-40% to reach confluency of 60-80% on the day of the exposure. The medium used was Ham's F-12K medium supplemented with 15% FBS, 1% P/S, 1% NEAA, 2 × 10−3 M l-gln. Right before observation under the microscope, Live Cell Imaging Solution was added (30% of total media volume) to the cell culture media to ensure long-term cell survival although the cells were maintained at 37°C in a 5% CO2 humidified atmosphere in a custom-built stage-top incubator. The plasma membrane of cells was labelled with 1 µg/ml Cellmask Orange for the duration of the experiment..

The cells were exposed to titanium dioxide nanotubes, labelled with Alexa647 [4] at a cell/tissue normalized surface dose 10:1 (ratio between the surface of nanoparticles and the cell growth area). Nanoparticles were aerosolized onto the living cells, which were covered with a thin layer (200 nm-500 nm) of cell media. The thin layer of water was achieved by removing most of the cell media right

before the exposure. Aerosolization was performed using Aeroneb Pro nebulizer that produces 4-6 µm sized drops.

Results

With a system simulating inhalation exposure in lungs, where titanium dioxide nanotubes (in red) were nebulized on top of living cells (in green) with only a thin layer of water on top, we were able to directly capture nanoparticles passing through the plasma membrane in matter of seconds. At time points exceeding 20 s, we can see nanoparticles also accumulating at the membrane, while still passing through it. We are able to see bare nanoparticles (just red color inside the cells) and membrane-coated nanoparticles (yellow color) inside and outside the cells. This fast entry of nanoparticles indicates that nanoparticles pass the membrane quickly, most probably caused by direct contact with the membrane. We propose the mechanism of entry to be nanoparticle wrapping – the direct interaction of the nanoparticle surface with membrane lipids.[5] This then also creates holes in the membrane through which other nanoparticles can pass the membrane bare.

Conclusions

By employing 3D-STED microscopy, we confirmed with 40 nm lateral and 500 nm axial resolution that nanoparticle pass over the cell membrane faster than in one second. This indicates that nanoparticles are able to enter living cells quicker than with the usual endocytotic biological uptake. This entry is quite possibly caused by direct interaction of NPs and cells, for example by nanoparticle wrapping into membrane lipids.[5]

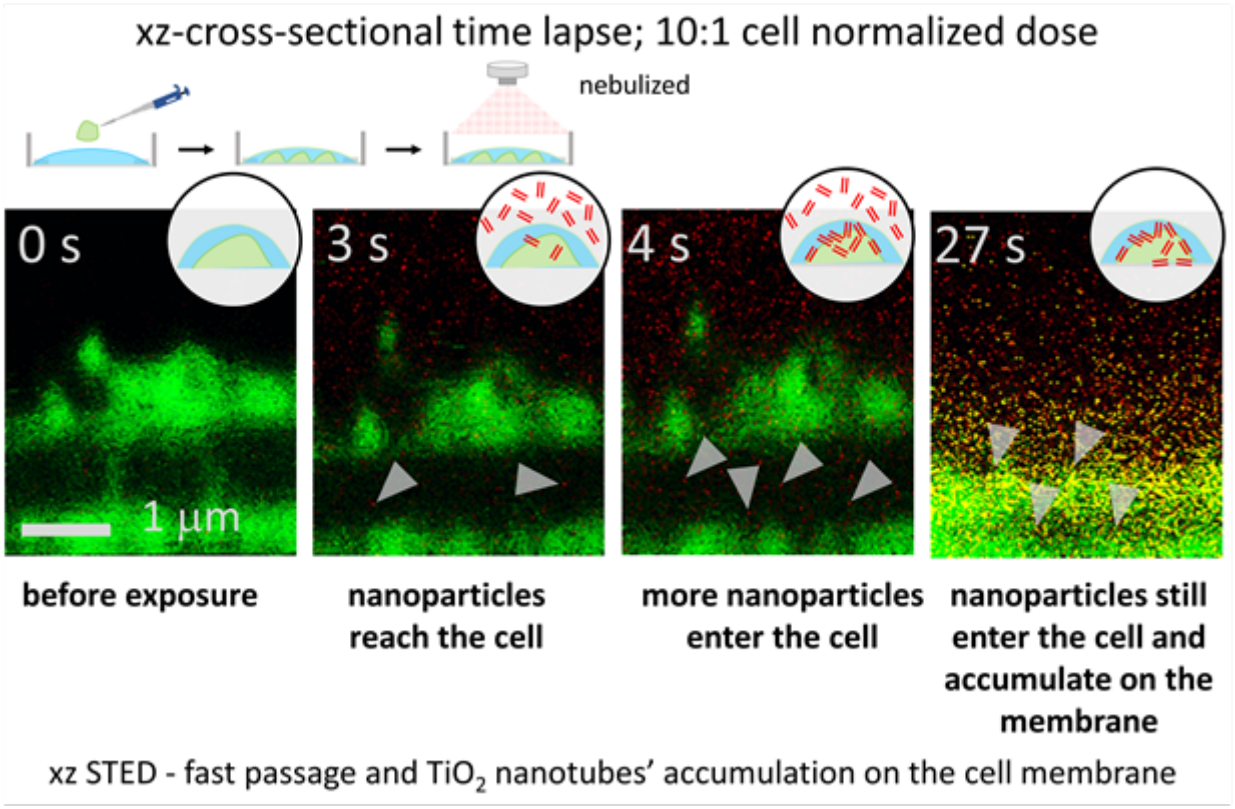

Keywords:

live-cell microscopy, nanoparticle tracking, 3D-STED

Reference:

1. N. Prajitha, S. S. Athira, P. V. Mohanan, Environmental Research. 172, 98–108 (2019).
2. G. Oberdörster, E. Oberdörster, J. Oberdörster, Environmental Health Perspectives. 113, 823–839 (2005).
3. S. Dasgupta, T. Auth, G. Gompper, Nano Lett. 14, 687–693 (2014).
4. B. Kokot et al., Nanotoxicology, 1–22 (2021).
5. I. Urbančič et al., Nano Lett. 18, 5294–5305 (2018).

830

Microscopic characterization of graphene derivates in life science

Mgr., Phd Zuzana Chaloupkova[1,2], Mgr. Jana Straska[1,2]
[1]Czech Advanced Technology and Research Institute - Regional Centre of Advanced Technologies and Materials, Olomouc, Czech Republic, [2]VSB Tech Univ Ostrava, IT4Innovations, Ostrava, Czech Republic

Poster Group 1

Background incl. aims
Graphene derivatives are becoming increasingly important materials in the field of biomedicine, particularly in neurosciences. Their ability to interact with cells and their potential applications in neuroapplications present an intriguing and revolutionary potential1. This study focuses on the microscopic characterization of various graphene derivatives with the aim of identifying the most suitable ones for neuroapplications, taking into account cell uptake and their biocompatibility. The objective of this study is to conduct microscopic characterization of graphene derivatives and evaluate their interaction with cellular structures. Specifically, we focus on their distribution within cells, cellular uptake, and biocompatibility.
Methods
Microscopic characterization of graphene derivatives was performed using several techniques, including the combination of scanning electron microscopy (SEM) with atomic force microscopy (AFM), transmission electron microscopy (TEM), high-resolution TEM (HR-TEM), time-lapse confocal microscopy and Raman spectroscopy. These methods allowed us to examine the morphology, structure, and interaction of derivatives with cellular structures.
Results
Our microscopic characterization revealed that different graphene derivatives exhibit distinct morphology and structure. Using SEM/AFM, we observed differences in particle size and shape. TEM and HR-TEM enabled detailed examination of the internal structure of derivatives. Time-lapse confocal microscopy will be employed to track the dynamic interaction of graphene derivatives with cellular structures over time, providing insights into their uptake kinetics, intracellular trafficking, and potential effects on cellular dynamics. Raman spectroscopy provided information about the chemical structure of derivatives. An important finding was that certain derivatives demonstrated higher cellular uptake and better biocompatibility than others.
Conclusion
Based on our results, microscopic characterization is crucial for selecting optimal graphene derivatives for neuroapplications. Certain derivatives exhibited significantly enhanced ability to interact with cells and higher biocompatibility, indicating their potential for use in neurosciences2. Further studies focusing on long-term effects and applications of these derivatives are necessary to assess their full therapeutic potential.

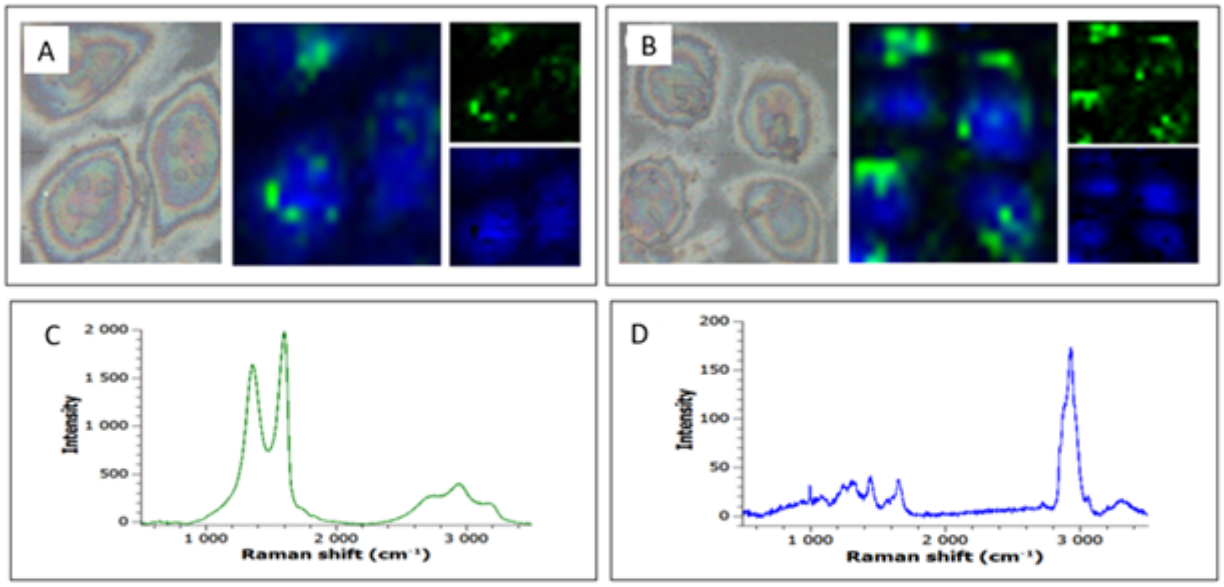

Figure 1: *Map of HeLa cells with GO incubation concentration of 18.75 µg ml^{-1}. The top left shows the microscope image with the mapping area marked, the top right shows the obtained RGB map (also for the individual components, i.e. GO and HeLa cell). Blue represents HeLa cells and green represents GO particles; B – HeLa cell map with GO concentration of 25 µg ml; C – Raman spectrum of GO, shown in green on the RGB map and D – Raman spectrum of HeLa cell, shown in blue on the RGB map. Note: the scale bars are 10 µm.*[3]

Keywords:

Graphene, cells, SEM/AFM, TEM, Raman

Reference:

1Nejabat M. et al. J Biomed Mater Res A. 105(8), 2355, 2017
2Su X. et al. Biosens Bioelectron. 92, 489, 2016
3Chaloupková et al., Analytical Methods, 15 (42), 5582-5588, 2023

862

Birefringence analysis of hemozoin with surface plasmon microscopy towards malarial species distinction

Dr. Ipsita Chakraborty[1], Prof. Andreas Offenhäusser[1]
[1]Forschungszentrum Jülich GmbH, Jülich,, Germany

Poster Group 1

I. Introduction

Female Anopheles mosquitoes carrying the Plasmodium parasite are the primary vectors of malaria mostly prevalent in countries exhibiting tropical climate [1]. The parasite species Plasmodium falciparum, Plasmodium vivax, Plasmodium malaria, Plasmodium ovale, and Plasmodium knowlesi are the five that can infect humans. Plasmodium falciparum is responsible for 70% of the infections, whereas Plasmodium vivax is responsible for 20% of them [1]. WHO reports that 249 million cases were recorded in 2022, of which 233 million (about 94%) were reported in Africa. Nearly half of all cases were reported in Nigeria (27%), the Democratic Republic of the Congo (12%), Uganda (5%), and Mozambique (4%). Malaria is expected to have caused 608,000 fatalities worldwide in 2022. Just four nations accounted for more than half of all deaths: Tanzania (4%), Niger (6%), the Democratic Republic of the Congo (12%), and Nigeria (31%). Eleven countries namely Burkina Faso, Cameroon, the Democratic Republic of the Congo, Ghana, India, Mali, Mozambique, Niger, Nigeria, Uganda, and Tanzania account for almost 70% of the world's malaria cases [2].

There exist many techniques for detection of malarial species. Conventional light microscopy involves examining blood smears with Giemsa stain has been the golden standard, while other techniques including rapid diagnostic test and polymerase chain reaction (PCR) have also been utilized. Most of these techniques require a long processing time and are not quantitative in general. Further, label free techniques are scarce in malarial detection.
This work is based on the anisotropic characterization of hemozoin utilizing surface plasmons. We explicitly studied the difference in the birefringence of whole blood with and without hemozoin.

II. Methods

Focused surface plasmon microscopy [3] is a technique that measures light-matter interaction at sub-wavelength level to investigate local optical properties of the sample at the metal-dielectric interface. It relies on optical near-field effects to map the refractive index profile of the samples with high spatial resolution. Numerous samples (i.e., thin films and liquids) have been probed (probe size:180 nm) by this technique to reveal circular absorption pattern at the exit pupil of the high numerical aperture microscope objective. By correlating the radius of the absorption pattern one can determine the refractive index of the sample. Further, anisotropic characteristics of the sample (if present) can be extracted from the elliptical absorption pattern to reveal the magnitude of birefringence and orientation of its fast axis respectively [4].
NLAF21 coverslips (refractive index: 1.78) were cleaned with ethanol, acetone, and isopropanol for 5 mins each. Then the coverslips were subjected to oxygen plasma for 5 mins. Then a chromium layer (~2 nm, r.i.: 3.316+i3.312) followed by gold layer (~ 47 nm, r.i.: 0.18377+i3.4313) were deposited by E-beam vapor deposition. The chromium layer was added for a better adhesion of the gold layer. The thickness of the subsequent layers was correlated with X-ray diffraction analysis. Artificial blood (~1 µl) was added on top of the substrate. Later various concentrations of hemozoin were mixed in the artificial blood and pipetted on top of the substrate.

III. Results

The reflected spatial frequency distribution at the exit pupil of the high numerical aperture objective lens was recorded. When artificial blood was used as sample, we observed a circular absorption pattern at the exit pupil plane indicating the absence of any anisotropic components. The refractive index was recorded from the radius of the circular absorption pattern with a semi-automated custom developed software. When hemozoin was mixed in artificial blood, we observed an elliptical absorption pattern at the exit pupil plane. The birefringence was extracted from these images with the developed software as stated before.

IV. Conclusion

In this proof-of-concept study, we conclude that refractive index and more so birefringence can be used as a label-free estimator differentiating healthy blood and malarial blood. Further this approach can be used to distinguish between various malarial species as reported previously based on the refractive index [5]. We believe the quantitative characterization of the hemozoin crystals from various plasmodium species could be used in future to easily distinguish the species.

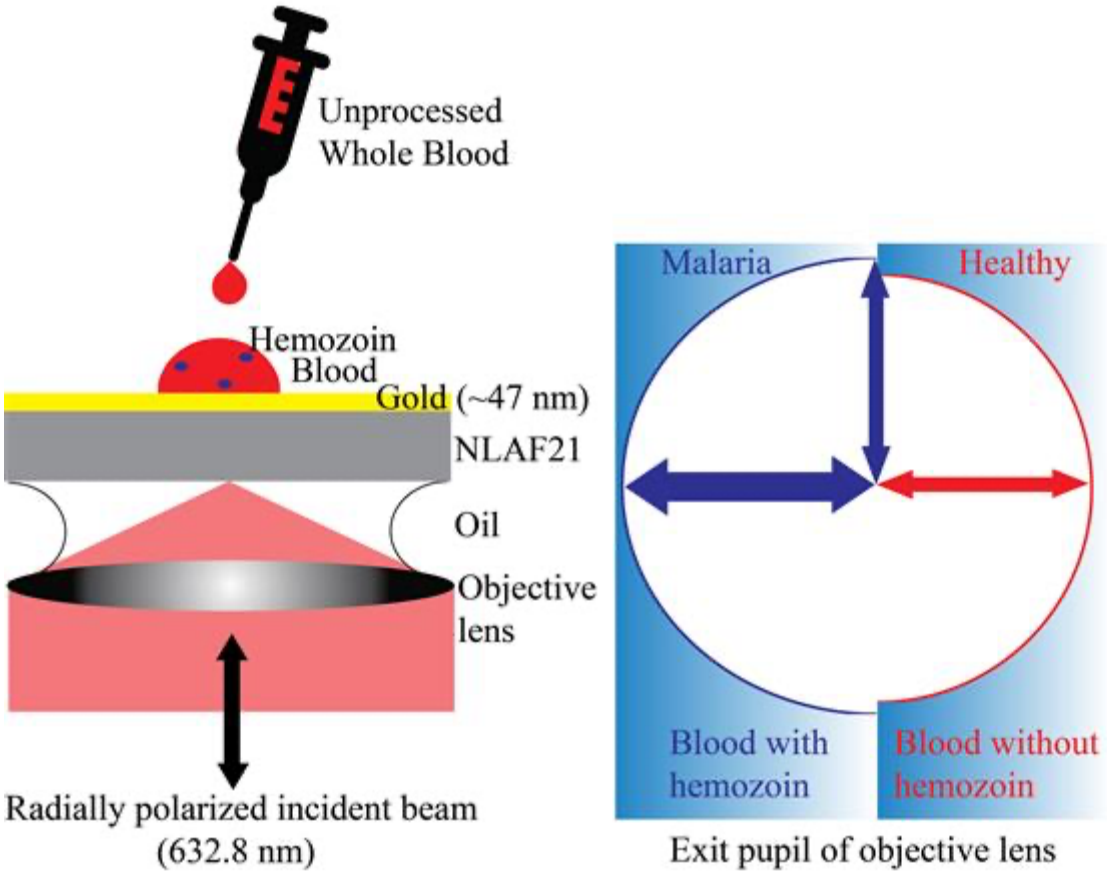

Keywords:

Label-free
Birefringence
Malaria
Surface plasmon

Reference:

[1] CDC Malaria, https://www.cdc.gov/dpdx/malaria/index.html
[2] Priya Venkatesan, “The 2023 WHO World malaria report”, The Lancet Microbe, 5(3), 214, (2024). https://doi.org/10.1016/S2666-5247(24)00016-8
[3] Ipsita Chakraborty and Hiroshi Kano, “Characterization of cellophane birefringence due to uniaxial strain by
focused surface plasmon microscopy”, OSA Continuum, 4, 409 - 415, (2021). 2021). https://doi.org/10.1364/OSAC.417743
[4] Ipsita Chakraborty and Hiroshi Kano, “Microscopic-characterization of photo-induced birefringence of azopolymer
thin film by focused surface plasmon”, Optics & Laser Technology, Volume 147, 107673, (2022). https://doi.org/10.1016/j.optlastec.2021.107673
[5] Ipsita Chakraborty, Justus Bednar and Andreas Offenhäusser, "Detecting malaria with surface plasmon microscope", Biophotonics in Point-of-Care III, Paper 13008-6 (2024).

872

Microscopy of body surface sculpturing in terrestrial crustaceans

Ana Žuran[1], Dr. Miloš Vittori[1]
[1]Department of Biology, Biotechnical Faculty, University of Ljubljana, Ljubljana, Slovenia

Poster Group 1

Background
Terrestrial isopods (Oniscidea) are a successful group of terrestrial crustaceans, partly due to their finely structured exoskeletal cuticle. The cuticle is an elaborate extracellular matrix deposited by epidermal cells and consists of several layers. The epicuticle, the thinnest and outermost layer, forms remarkably diverse and complex structures, such as scales and other micrometre-sized ornaments that influence the surface properties of the cuticle and the interaction of isopods with their environment [1, 2]. However, not much is known about the formation of the epicuticle and these structures. The aim of this study was to develop a simple protocol to investigate dorsal epicuticle formation in terrestrial isopods during molt. For this purpose, a combination of scanning electron microscopy (SEM) and confocal laser scanning microscopy (CLSM) was applied to image the deposition of the new epicuticle during molt in the terrestrial isopod Porcellio scaber.
Methods
Tergites of P. scaber specimens in different stages of cuticle deposition during preparation for molt [3] were dissected, fixed in a mixture of paraformaldehyde and glutaraldehyde, and decalcified with EDTA. For SEM imaging, the samples were osmicated and embedded in paraffin. At this stage, the old cuticle was cut off with a razor blade to expose the ecdysial space for observation. Paraffin was then removed, and samples were air-dried in hexamethyldisilazane and sputter-coated with platinum. Prepared samples were imaged using a JSM-7500 field emission scanning electron microscope (JEOL). For CLSM imaging, the decalcified samples were incubated in methyl green, a far-red emitting fluorescent DNA dye, to visualize cell nuclei [4]. Subsequently, the samples were cleared and mounted in ProLong™ Glass Antifade Mountant (Invitrogen). Series of optical sections were acquired using a Stellaris 8 confocal microscope (Leica).
Results and conclusions
Using the described procedure, we were able to expose the ecdysial space and the surface of the epidermis and observe the new epicuticle in different stages of its formation with SEM from a perspective never seen before. In the late stage of cuticle deposition, we observed the fully sculptured new epicuticle with numerous scales and sensory tricorns (Fig. 1A), whereas in the early stage, the surface of the underlying epidermis was exposed, showing stubby apical cell membrane protrusions and only the outlines of the edges of new scales. Using CLSM, we were able to observe cuticle autofluorescence in relation to DNA-bound methyl green fluorescence and thus determine the position of epidermal cells in relation to the position of emerging epicuticular structures (Fig. 1B). In this way, we established that each scale is likely deposited by a single epidermal cell. The presented protocol allowed us to observe the complex architecture of the epicuticle during its deposition and to gain information about the mechanism of epicuticular sculpturing by the epidermal cells that secrete it. In the future, we plan to extend this protocol by analysing the changes in epidermal cell ultrastructure during epicuticle formation using transmission electron microscopy.

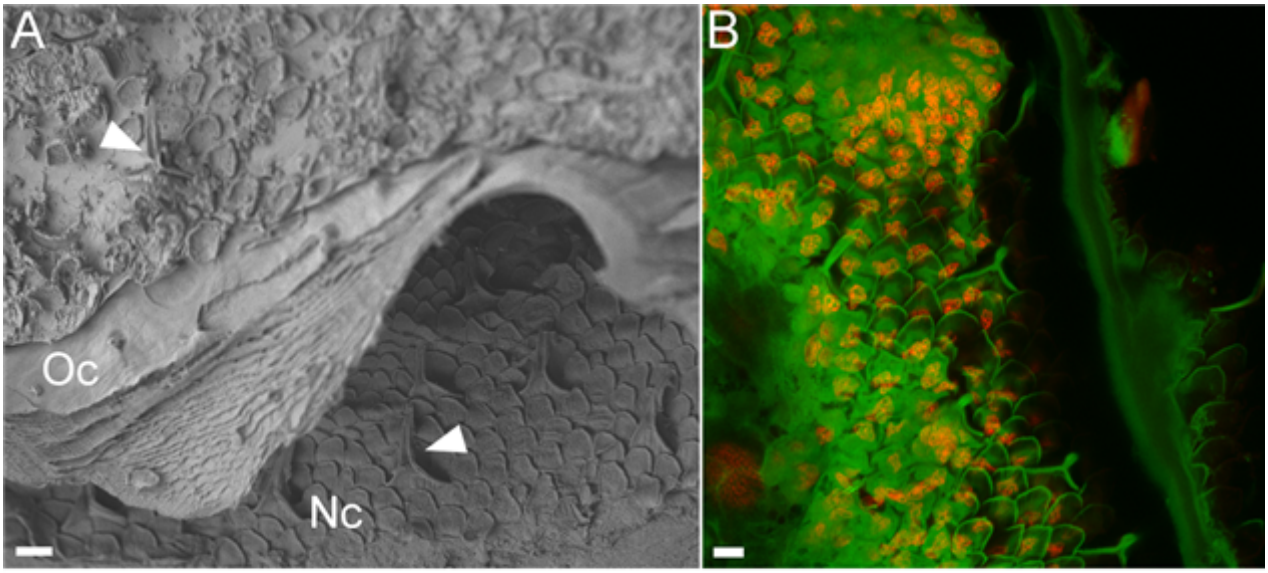

Figure 1. Tergites during the late stage of cuticle deposition. **A)** SEM micrograph showing the surface of the old (Oc) and new (Nc) cuticle during preparation for molt. Numerous scales and sensory tricorns (arrowheads) are visible on both cuticular surfaces. Scale bar = 10 µm. **B)** Overlay of optical sections imaged with CLSM showing the surface of the new cuticle (green) with scales and the position of the nuclei of the underlying epidermal cells (red). Scale bar = 10 µm.

Keywords:

arthropods, cuticle, SEM, CLSM

Reference:

1. S. Sfenthourakis, S. Taiti, Zookeys, 515 (2015)
2. H. Schmalfuss, Zoomorphologie, 91 (1987)
3. P. Zidar, D. Drobne, J. Štrus, Crustaceana, 71 (1998)
4. M. Vittori, M. Khurshed, D. I. Picavet, C. J. F. van Noorden, J. Štrus, Arthropod Struct. Dev., 47 (2018)

902

Mechanisms of microglial responses to injury related focal ATP events

Dr Zsuzsanna Környei[1], Péter Berki[2,5,6], Dr Csaba Cserép[1], Dr Nikolett Lénárt[1], Dr Balázs Pósfai[1], Balázs Kalmár[1], Dr Kaikai He[3], Dr Ya Wang[4], Dr Zhaofa Wu[3], Dr Yulong LI[3], Dr Miao Jing[4], Dr Ádám Dénes[1]

[1]Momentum Laboratory of Neuroimmunology, Institute of Experimental Medicine, Budapest, Hungary, [2]János Szentágothai Doctoral School of Neuroscience, Semmelweis University, Budapest, Hungary, [3]State Key Laboratory of Membrane Biology, New Cornerstone Science Laboratory, School of Life Sciences, Peking University, Beijing , China, [4]Chinese Institute for Brain Research, Beijing , China, [5]Laboratory of Cerebral Cortex Research, Institute of Experimental Medicine, Budapest, Hungary, [6]Laboratory of Neuronal Network and Behaviour, Institute of Experimental Medicine, Budapest, Hungary

Poster Group 1

Microglia, the main immunocompetent cells in the central nervous system, rapidly respond to disturbances in their microenvironment, largely relying on purinergic (ATP, ADP) signaling through P2Y12 receptors. However, while the effects of exogenous ATP on microglial activity have been extensively tested in previous studies, the mechanisms involved in microglial response to endogenous, focal ATP events in the brain tissue are unclear. To visualize changes in the extracellular ATP levels, we introduced a sensitive fluorescent ATP sensor (GRAB-ATP) to cultured neurons and astrocytes and prepared acute brain slices from mice expressing the sensor in VGlut1+ neurons. We observed both spontaneous and injury-related ATP events in astrocytes and neurons in vitro, and detected significant extracellular ATP increase after slice preparation or secondary injury, even hours after slice cutting. ATP accumulation due to blockade of ecto-ATPase activity indicated an ongoing ATP release from the damaged tissue. Interestingly, we also observed a highly dynamic, focal, flashing ATP activity, persisting for hours ex vivo. Importantly, microglia processes were recruited to complex, nano- and micromolar ATP events in a P2Y12R and CX3CR1 dependent way, leading to marked morphological transformation of the cells. Microglial response to spontaneous- and injury-related ATP signals also occurs in vivo as revealed by in vivo two-photon microscopy. We suggest that focal, submilimolar ATP events represent a major modulator of microglial states and are likely to alter inflammatory responses in different CNS disorders.

Keywords:

ATP, microglia, acute brain slice

Reference:

1. Wu, Z., He, K., Chen, Y., Li, H., Pan, S., Li, B., Liu, T., Xi, F., Deng, F., Wang, H., Du, J., Jing, M., & Li, Y. (2022). A sensitive GRAB sensor for detecting extracellular ATP in vitro and in vivo. Neuron, 110(5), 770-782.e5. https://doi.org/10.1016/j.neuron.2021.11.027
2. Chen, Y., Luan, P., Liu, J., Wei, Y., Wu, Z., & Jing, M. (2022). Spatiotemporally selective ATP events from astrocytes encode injury information and guide sustained microglial response. (p. 2022.06.21.497103). bioRxiv. https://doi.org/10.1101/2022.06.21.497103
3. Berki, P., Cserép, Cs., Balázs Pósfai, B., Szabadits E., Környei Zs., Kellermayer A., Nyerges, M., Wei X., Mody I., Araki K., Beck H., He K., Wang Y., Wu Z., Jing M., Li Y., Gulyás AI. & Dénes Á. Microglia undergo rapid phenotypic transformation in acute brain slices but remain essential for neuronal synchrony. bioRxiv. https://doi.org/10.1101/2022.04.12.487998

941

Mapping of phase separation of supramolecular protein assemblies by live-cell holotomography microscopy

Dr Orlando Marin[1], Dr Arina Dalaloyan[1], Professor Michael Elbaum[1]
[1]Weizmann Institute of Science, Rehovot, Israel

Poster Group 1

Supramolecular protein assemblies (SMPAs) have demonstrated to be a great tool for studying the biophysical properties of human cells. Liquid-liquid phase separation is a driving mechanism in the assembly of various intracellular structures. An oligomerizing biomimetic system, known as Corelets, has helped to map phase separation within the cell subregions by means of protein condensation. Corelets are photosensitive phase-separating photoinduced oligomers of self-interacting proteins. Previous studies on protein condensation by localized oligomerization showed that sequestering protein ligands to slowly diffusing nucleation centers move the cell into different regions of the phase diagram, resulting in localized phase separation. The real-time oxidative-induced stress in human cells has also remained an enigma in cellular biology. A previous work on the redox state of the cell showed that supramolecular protein assemblies have a self-assembly interface sensitive to the exposure to a thiol-specific oxidizing reagent. We worked with a system of self-associating proteins built onto a ferritin core, genetically encoded for the expression of supramolecular protein assemblies based on a fusion construct between citrine, a yellow fluorescent protein variant and the heavy chain human ferritin. Here, we use a novel 3D label-free non-invasive fluorescent live-cell imaging method, which allows performing high-precision in-vivo holotomographic microscopy of subcellular structures, coupled with cryo-electronic tomography and image processing to evaluate real-space structure of solid and liquid localized phase separation and of SMPA oxidation within the cell nucleus; which allows us to use the refractive index as a method to map the emergence and prevalence of the Corelets in the cells. Our work has allowed the three-dimensional visualization of phase separating condensates in mammalian cells.

Keywords:

Protein condensation, label-free, refractive index

Reference:

1. Giuliano, B. et al, Angew. Chem. Int. Ed., 2014, 53, 1534 –1537.
2. Bracha, D. et al, Cell, 2018, 175, 1467–1480.
3. Giuliano, B. et al, Nano Lett., 2016, 16, 6231−6235.
4. Giuliano, B. et al, Biomacromolecules, 2015, 16, 2006−2011.

944

Enhanced sensitivity in label-free live-cell imaging using multi-pass stimulated Raman scattering microscopy

Joshua Reynolds[1], Dr. Shaun Burd[1], Tzu-Chieh (Jerry) Yen[1], Dr. Samsuzzoha Mondal[1,2], Dr. Soichi Wakatsuki[1,2], Dr. Mark Kasevich[1]
[1]Stanford University, Stanford, USA, [2]SLAC National Accelerator Laboratory, Menlo Park, USA

Poster Group 1

Background incl. aims
Stimulated Raman scattering (SRS) microscopy is a label-free imaging technique used for measuring chemical concentrations with high spatial resolution. The chemical sensitivity of SRS microscopy is limited by photostress or photodamage in sensitive specimens or by the timescales of fast dynamics. To increase the signal-to-noise and thus the sensitivity of SRS microscopy in live samples, we implement a multi-pass imaging protocol.

Methods
Two femtosecond near-infrared laser beams—a pump beam and a Stokes beam—are used to drive SRS. Pulses from both beams are chirped to gain spectral resolution in the measurements [1]. A Pockels cell is used to rotate the polarization of the Stokes pulses, first to initiate and then to end the multi-pass process. An intensity modulation on the pump beam results in a time-varying intensity gain in the multi-passed Stokes beam due to SRS, which is detected with a lock-in amplifier.

Results
We demonstrate an enhanced signal-to-noise ratio in SRS measurements at constant optical dose relative to equivalent single-pass measurements in both spectroscopy and imaging, with signal-to-noise increases currently of about 6 dB. We further characterize the performance of the microscope as a function of the number of interactions between the Stokes pulse and the sample and numerically study the tradeoffs and optimal operating conditions for multi-pass imaging. Using this microscope, we image live biological targets including plant roots and nematodes and use the chemical specificity of SRS to differentiate important biomolecules with subcellular spatial resolution.

Conclusion
Multi-pass protocols enable higher signal-to-noise measurements and thus increased sensitivity or imaging speed, as we demonstrate here for label-free live-cell imaging in an SRS microscope. Multi-pass techniques can be used to increase the sensitivity of many dose-limited measurements up to fundamental quantum limits [2, 3]. We show that multi-passing overcomes the shot-noise-limited signal-to-noise ratio of a standard single-pass experiment conducted with the same total optical dose. This increased sensitivity could enable new measurements of the spatial distribution of low-concentration or weakly scattering molecules in dose-sensitive biological specimens without the need for disruptive labels.

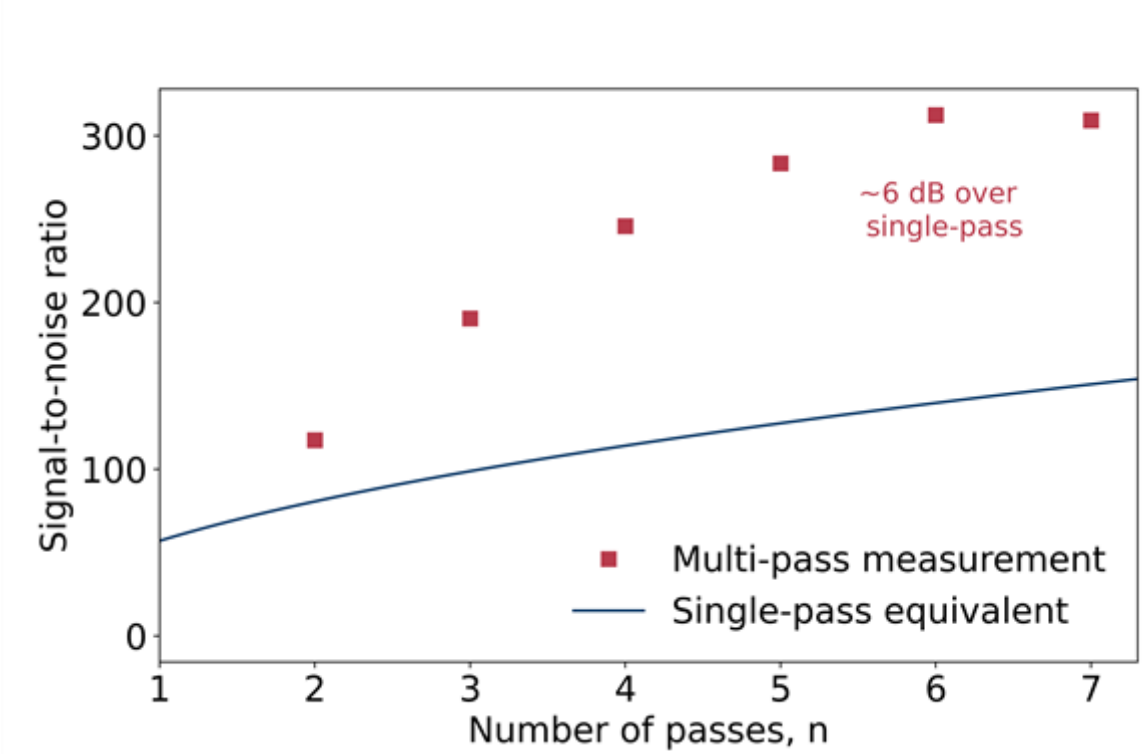

Keywords:

Label-free, stimulated Raman scattering

Reference:

[1] E. R. Andresen, P. Berto, and H. Rigneault, Stimulated Raman scattering microscopy by spectral focusing and fiber-generated soliton as Stokes pulse. Optics Letters 36, 2387 (2011).
[2] V. Giovannetti, S. Lloyd, and L. Maccone. Quantum Metrology. Physical Review Letters 96, 010401 (2006).
[3] Y. Israel, J. L. Reynolds, B. B. Klopfer, and M. A. Kasevich. Continuous wave multi-pass imaging flow cytometry. Optica 10, 491 (2023).

952

Temporal analysis of bone development in chick femur bone using label-free imaging

Miss Siddhi Chugh[1], Mr Jacob Kleboe[1,2], Dr Rahul S. Tare[3], Professor Richard OC Oreffo[2,3], Professor Sumeet Mahajan[1,2]
[1]School of Chemistry, Southampton, United Kingdom, [2]Institute of Life Sciences, Southampton, United Kingdom, [3]Human Development and Health, Southampton, United Kingdom

Poster Group 1

Background incl. aims:
Long bones such as femur develop via the process of endochondral ossification (EO). During EO, chondrocytes proliferate, undergo hypertrophy and subsequent cell death with the replacement of hyaline cartilage with bone. The constructed cartilaginous matrix is invaded by blood vessels, osteoblasts, osteoclasts, and bone marrow cells before it develops into bone. Currently, the gold standard techniques to study organ development are micro computed tomography, histochemical assays, or through fluorescence microscopy using dyes or endogenously expressed fluorescent proteins protein. However, all these approaches are invasive, and can require fixation or lysis of tissue, therefore are unsuitable for in-vivo studies on humans for monitoring disease progression or therapeutic benefit.
However, multiphoton microscopy utilising non-ionising, benign radiation (NIR light) offers non-invasive, label-free structural and chemical details, without damage in contrast to histological approaches and X-ray scans. Additionally, label-free microscopy facilitates high sensitivity and resolution. In this work, we report an application of multiphoton microscopy with the techniques of Second Harmonic Generation (SHG), Coherent Anti-Stokes Raman Scattering (CARS) and 2-Photon Excited Auto-Fluorescence (2PaF) to monitor bone development. We establish the methodology using the chick model to provide proof-of-concept of its capability for potential use with patients.
Methods:
The femurs of chick embryos were isolated at different growth phases, i.e., at day 11, 14, and 18. The bones were fixed, embedded in paraffin wax, and sectioned. The sectioned slices were imaged with histological methods to establish the ground truth. The parallel sections were imaged with SHG, CARS and 2PaF. SHG images collagen fibres while CARS is used to image distribution of lipids at their vibrational frequency of 2845cm-1 and 2PaF images autofluorescence at 520 nm (primarily FAD and NADH). CARS was obtained in both backward and forward scattering geometries. Subsequently, label-free imaging data was analysed using image analysis using Fiji software. SHG images were analysed using CT-FIRE software and statistical analysis were performed.
Results:
Histological staining (Alcian Blue and Sirius Red) revealed a clear demarcation between the early cartilaginous femur and the surrounding tissue. Proteoglycans were visible within the cartilage region and intense collagen staining in the tissue surrounding the femur.
SHG images of chick femur bones (n=6) at Day 11, 14 and 18 highlighting collagen fibres were analysed using “CT-FIRE” to extract collagen fibre details. It was observed that the length of collagen fibres steadily increased throughout the developmental process from Day 11 to Day 18, unlike the fibre width that remained similar for early developmental stages before sudden increase at day 18. However, there were no observed differences in fibre straightness throughout the developmental process. 2PaF images provided context for cells and tissue areas while CARS images showed the distribution of lipids and protein structures and provided a readout of changes on development from Day 11 to 18. Further analysis is in progress to develop imaging based multimodal signatures for bone development.

Conclusions:
Our work shows that non-invasive and non-destructive, structurally, and chemically selective multiphoton label-free imaging techniques can be advantageous for monitoring bone formation and can track its development. Additionally, the label-free techniques explored here allow objective and quantitative analysis of the developing bone since signals are retrieved only from molecules and structures in their native state providing intrinsic contrast and are dependent on their amounts.

Keywords:

Bone development, Multiphoton-microscopy, label-free imaging,

Reference:

1. Fu R, Liu C, Yan Y, Li Q, Huang R-L. Bone defect reconstruction via endochondral ossification: A developmental engineering strategy. Journal of Tissue Engineering. 2021;12. doi:10.1177/20417314211004211
2. Shin, K. S., Men, S., Wong, A., Cobb-Bruno, C., Chen, E. Y., & Fu, D. (2022). Quantitative Chemical Imaging of Bone Tissue for Intraoperative and Diagnostic Applications. Analytical Chemistry, 94(9), 3791-3799. https://doi.org/10.1021/acs.analchem.1c04354
3. Boudaoud, A., Burian, A., Borowska-Wykręt, D., Uyttewaal, M., Wrzalik, R., Kwiatkowska, D., & Hamant, O. (2014). FibrilTool, an ImageJ plug-in to quantify fibrillar structures in raw microscopy images. Nature Protocols, 9(2), 457-463. https://doi.org/10.1038/nprot.2014.024
4. Fussell, A., Isom‰ki, A., & Strachan, C. (2014). Nonlinear Optical Imaging Introduction and Pharmaceutical Applications. ChemInform, 45, 54-63.

987

Non-toxic clearing and labeling with fluorescent REAfinityTM antibodies for enhanced 3D visualization of tissues

Msc Kevin Bigott[1]
[1]Miltenyi Biotec B.V. & Co. KG, Cologne, Germany

Poster Group 1

Background
Generation of a 3D cellular topography of biological specimens is often essential to understand cellular and molecular processes. Especially, spatial visualization of heterogenous protein expression in solid tumor samples is considered important for advanced phenotyping and potential diagnostic applications. However, for a long time, biologists were limited to the visualization of thin tissue sections, which provides limited cellular context. Furthermore, sectioning is time-consuming and often prone to artifacts, like ripping and folding. While clearing methods in combination with light-sheet fluorescence microscopy have emerged as powerful tools for 3D reconstruction of tissues, most clearing techniques involve toxic reagents which require special safety provisions and generate extra effort for sample preparation as well as imaging. To address these shortcomings, we developed a clearing workflow based on non-toxic reagents that allows for efficient 3D imaging biological samples in combination with directly labeled REAfinityTM antibodies.
Methods
Briefly, samples were fixated with paraformaldehyde and permeabilized to facilitate delipidation and antibody-conjugate penetration during subsequent immunostaining. Whole-mount immunostaining was performed using REAfinityTM antibodies coupled to Vio® dye variants. Duration of the immunostaining depends on the tissue size and tissue type, ranging from 2 - 7 days. After staining, tissues were dehydrated using an ascending ethanol series. Subsequently, refractive index matching was performed; a process referred to as tissue clearing renders opaque tissues transparent and thereby improves optical light penetration depth. For blood-rich organs and tissues a carbamide peroxide based depigmentation module was applied to remove residual blood to facilitate increased light penetration during imaging. In addition, tertiary butanol and pH adjustment during dehydration and clearing process can be used to ensure preservation of endogenous fluorescent proteins. Imaging of large samples was performed using the UltraMicroscope Blaze light-sheet imaging platform. To eliminate noise, intensity inhomogeneities, striping artifacts and to enable deconvolution of imaging data, a postprocessing pipeline based on MACS® iQ 3D Large Volume software was applied.
Results
Our workflow enables 3D imaging of various biological samples, including mouse brain, lymph nodes, lung, intestine, liver, spleen, kidney, stem cell-derived organoids, xenografts, patient-derived tumor samples and tumor spheroids. To enable the effective clearing for blood-rich organs and tissues, an efficient depigmentation module was integrated to increase light transmission. Additionally, the protocol can be also modified to ensure preservation of endogenous fluorescence. For optimal 3D imaging, we combined the clearing procedure with whole-mount immunostaining of mouse tissues, human tumor samples and organoids using Miltenyi Biotec's REAfinityTM antibodies coupled to newly developed Vio® dye variants optimized for application in light-sheet microscopy. REAfinityTM antibodies are recombinant antibodies engineered to provide high specificity, purity, and superior lot-to-lot consistency compared to hybridoma-derived antibodies, whereas Vio® dyes are a new generation of fluorescent dyes characterized by remarkable brightness, photostability and highly resistant against organic solvents during clearing procedure. UltraMicroscope Blaze light-sheet imaging platform enabled fast high resolution imaging of large samples. Our data indicates highly

efficient labeling of the vasculature, different neuronal subtypes in mouse brains, as well as bright staining of neural progenitors and proliferative cells in cerebral organoids. Furthermore, carcinoma cells and lymphocytes were visualized in solid tumors and mouse lymph nodes, respectively. After data acquisition, a profound postprocessing pipeline based on the MACS® iQ 3D Large Volume software enables the elimination of noise, intensity inhomogeneities, striping artifacts and features deconvolution of imaging data, which ensures ideal preparation of 3D data for subsequent data visualization and quantification.

Conclusion

We present a robust, fast, flexible and non-toxic clearing procedure that allows for efficient 3D imaging of a wide range of biological samples. Optional modules for depigmentation of blood-rich organs and preservation of endogenous fluorescence can be applied in order to extend the procedure to applications with further requirements. By combining the advantages of REAfinityTM antibodies and Vio® dyes, we developed staining reagents that significantly reduce staining duration and are thus ideally suited for whole-mount tissue labeling, multiplexing, and imaging with light-sheet microscopy using the UltraMicroscope Blaze. Taken together, we developed an efficient clearing procedure combined with highly specific antibody conjugates and a data postprocessing pipeline for optimal 3D visualization of tissue and whole organs, paving the way for a better understanding of tissue structures and disease mechanisms. Extension of the clearing procedure for additional applications and constant development of further antibody conjugates coupled to additional Vio® dye variants will further increase marker coverage and the range of applications.

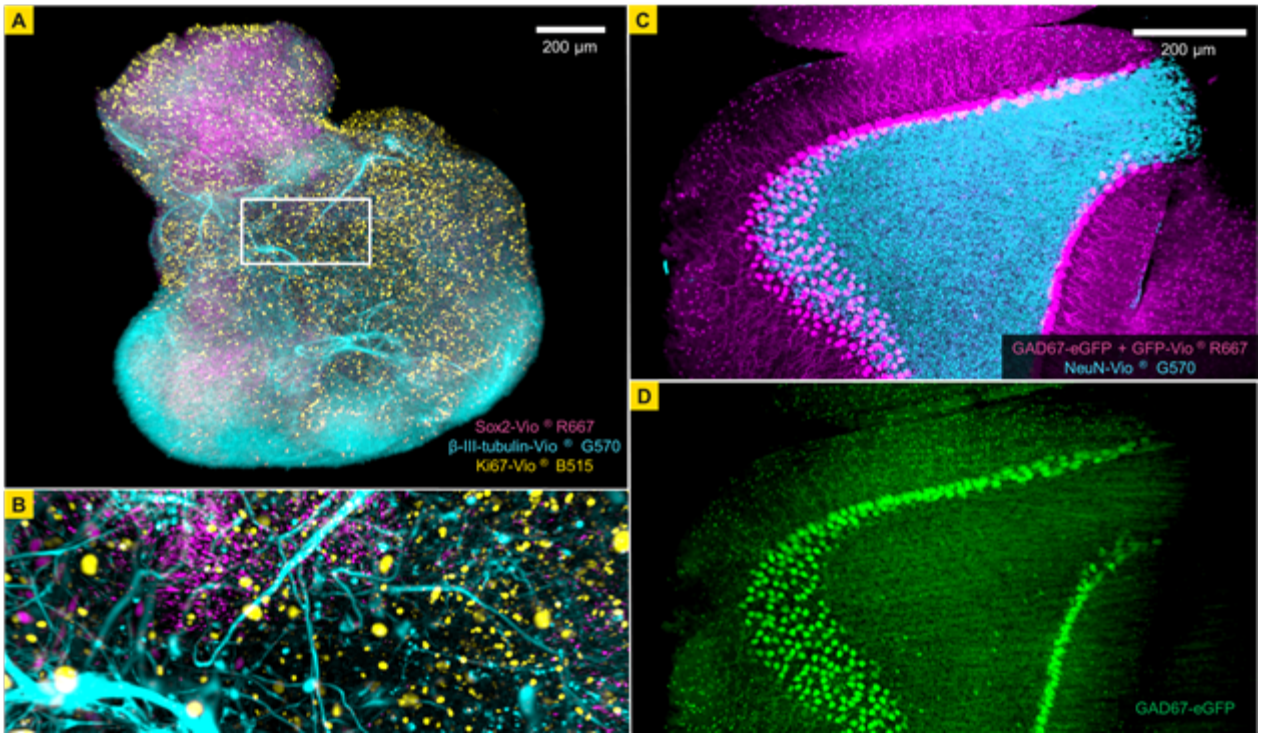

Keywords:

Tissue Clearing, 3D-IF, Ultramicroscopy, Lightsheet

1040

Ex Vivo Metabolic Imaging for Parotid Tumors: Implications for Precise Diagnosis and Customized Treatment

Phd Student Alessia Riente[1,2], Dr Alessio Abeltino[1,2], Dr Cassandra Serantoni[1,2], Dr Michele Maria De Giulio[1,2], Dr Duaa Hatem[1,2], Prof Marco De Spirito[1,2], Dr Mariaconsiglia Santantonio[3], Dr Michela Sollazzo[2], Dr Lela Calò[2], Prof Giulio Cesare Passali[2], Dr Jacopo Galli[2], Prof Giuseppe Maulucci[1,2]
[1] Catholic University of the Sacred Heart, Rome, Italy, [2]Fondazione Policlinico Universitario A. Gemelli IRCCS, Rome, Italy, [3]Ospedale Pediatrico Bambino Gesù, Rome, Italy

Poster Group 1

Background incl. aims
Primary parotid neoplasms necessitate specialized attention due to their diverse histological and clinical features [1,2]. Accurate classification and treatment selection rely on a thorough comprehension of both the phenotypic and molecular attributes of these tumors. Molecular markers and interactions within the tumor microenvironment critically influence their behavior. Therefore, identifying new markers using routine techniques such as needle aspiration to visualize tissue metabolism in vivo is essential for refining diagnostic accuracy and treatment strategies. Our study aims to preliminarily delineate the complex metabolic profiles of parotid gland tissues, especially focusing on distinguishing between healthy subjects and patients with squamous cell carcinoma, employing both Fluorescence Ratio (FRIM) and Fluorescence Lifetime (FLIM) Imaging Microscopy for precise quantification.

Methods
In our investigation, we conduct ex vivo analysis using advanced two-photon metabolic imaging techniques to examine the morphological, molecular, and functional aspects of parotid neoplasms. Fine needle aspiration biopsy is utilized to obtain cells for analysis, bypassing the need for invasive procedures and minimizing patient discomfort. Through this approach, we analyze metabolic markers such as NADH and FADH2, employing Fluorescence Ratio Imaging Microscopy (FRIM) and Fluorescence Lifetime Imaging Microscopy (FLIM) for precise quantification [3].

Results
Through the application of Metabolic Imaging techniques to analyze NADH and FADH2 levels in ex vivo samples, our objective is to complement traditional morphological assessments with a comprehensive evaluation of tissue metabolic states. We employed both microscopy imaging techniques to analyze the behavior of these two molecules in both healthy and diseased subjects. For instance, in the case of FRIM, we introduced an innovative workflow pipeline (depicted in Figure 1), which commences with autofluorescence imaging to derive redox ratio images by analyzing the blue and red channels. A redox ratio value approaching 0 indicates a state of reduction, while nearing 1 signifies oxidation. Subsequently, mitochondrial and cytoplasmic masks are applied to these images, enabling the assessment of tissue metabolic activity.

Figure 2 displays images in the blue channel, red channel, and the RR image generated by the analysis pipeline respectively for the healthy subject (top) and the subject affected by squamous cell carcinoma (bottom). These latter images feature a scale bar indicating areas of heightened metabolic activity within the tissue.

As shown in Figure 3, controls exhibit higher RR_mit values compared to patients, suggesting greater oxidative activity in healthy tissue.
RR_mit indicates the balance between reduced and oxidized pixels in relation to mitochondria, reflecting metabolic activity and cell viability. A higher RR suggests greater metabolic activity and more viable cells, while a higher RR low may signal metabolic alterations, as observed in squamous cell carcinoma. So, the higher RR_mit in healthy subjects compared to patients highlights significant disparities in tissue metabolic health.

We delved into metabolic dynamics by identifying the quantity of mitochondria exhibiting reduced and oxidized states within both healthy and diseased tissue, leveraging suitable algorithms for precise analysis.

Conclusion
Introduction of an innovative pipeline for autofluorescence image analysis has yielded significant findings. Notably, the results reveal a distinct contrast between healthy and diseased tissues. Moving forward, these insights are poised to influence diagnostic protocols and personalized treatments, with a focus on enhancing patient well-being. Such advancements hold promise for refining our understanding of tissue pathology and optimizing therapeutic strategies tailored to individual patient needs.

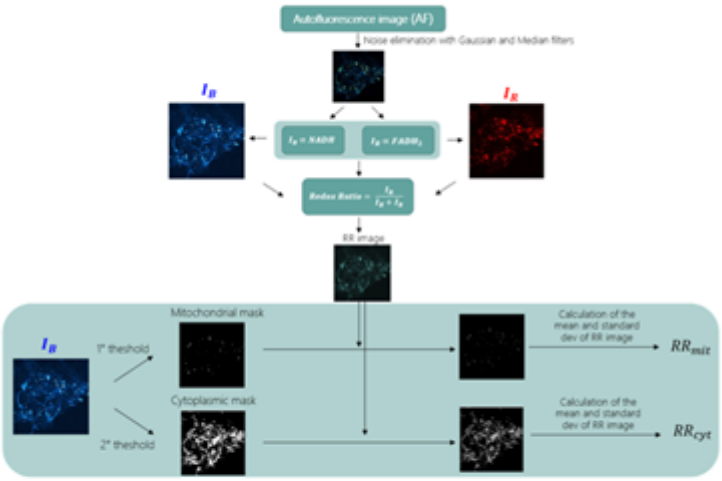

Figure 1. Workflow for clinical samples analysis

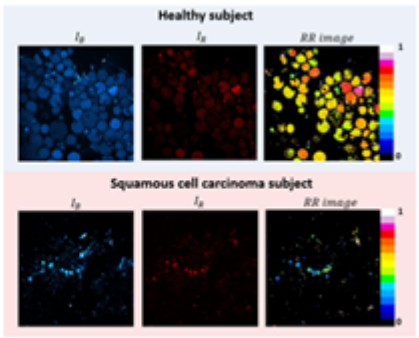

Figure 2. I_B, I_R and RR images for control and patient

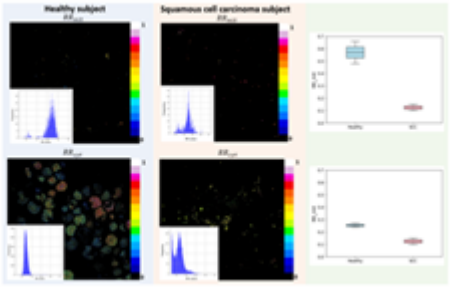
Figure 3. RR images results for control and patient

Keywords:

Metabolic Imaging, parotid carcinomas,metabolic markers

Reference:

[1] To, Victor Shing Howe, et al. "Review of salivary gland neoplasms." International Scholarly Research Notices 2012 (2012).
[2] Zbären, Peter, et al. "Carcinoma of the parotid gland." The American journal of surgery 186.1 (2003): 57-62.
[3]Bianchetti G, Ciccarone F, Ciriolo MR, De Spirito M, Pani G, Maulucci G. Label-free metabolic clustering through unsupervised pixel classification of multiparametric fluorescent images. Anal Chim Acta. 2021 Mar 1;1148:238173. doi: 10.1016/j.aca.2020.12.048. Epub 2020 Dec 31. PMID: 33516373.

1080

CAR T cell dynamics in a 3D collagen matrix: migration and interactions with cancer cells

Nicoline Dorothea Daugaard[1], Mike Bogetofte Barnkob[2], Zelvera Ismetova Usheva[2], Torben Barington[2], Jonathan R. Brewer[1]
[1]Department of Biochemistry and Molecular Biology, University of Southern Denmark, Odense, Denmark, [2]Centre for Cellular Immunotherapy of Haematological Cancer Odense (CITCO), Department of Clinical Immunology, Odense University Hospital, University of Southern Denmark, Odense, Denmark

Poster Group 1

Background incl. aims
Chimeric antigen receptor (CAR) T cell therapy is a therapy in which T cells are engineered to target a specific antigen on a cancer cell and elicit a T cell response that ultimately leads to the death of the cancer cell. CAR T cell therapy has proven effective against blood cancers, but solid tumors are more difficult and complex targets due to their tumor microenvironment. In order to develop efficient CAR T cell therapies against solid tumors, we need systems in which we can study, challenge, and improve CAR T cells in extracellular matrix-like 3D environments. Here, we have developed a 3D model based on rat tail collagen to study CAR T cells and their interactions with cancer cells.

Methods
We used CD19 CAR T cells, i.e. T cells targeting CD19 antigen, and A375 melanoma cells engineered to express the CD19 antigen. CAR T cells and cancer cells were mixed into a rat tail collagen matrix and spinning disk microscopy was used to record 3D time-lapse videos of the cells. We developed a quantitative 3D analysis and analyzed the T cell tracks to elucidate the migration of T cells and their interactions with cancer cells. We furthermore conducted a 72-hour treatment of mature melanoma spheroids using CAR T cells to investigate the efficiency of the therapy in the 3D collagen matrix. In all experiments, we compared with untransduced T cells, i.e. normal T cells that do not express the CD19 CAR.

Results
Our analysis of CAR T cell migration in the collagen matrix showed that CAR T cells generally move slower compared to untransduced T cells. While they both have the same number of interactions with cancer cells, CAR T cells tend to interact longer.
72-hours treatment of melanoma spheroids with CAR T cells in the collagen matrix resulted in a substantial reduction in spheroid growth. Spheroids treated with untransduced T cells increased in size comparable to untreated spheroids. These results demonstrate the efficacy of CAR T cells in targeting cancer tumors in the 3D collagen matrix.

Conclusion
We have successfully employed time-lapse imaging and quantitative 3D analysis to study the migration of CAR T cells and their interactions with cancer cells. We propose that the 3D model and the quantitative analysis presented here can be used to test various CARs, antigens, solid tumor types, and matrix modifications.

Keywords:

CAR, collagen matrix, time-lapse, migration

1115

Investigating nanoparticle interactions with the human blood-brain barrier in vitro

Hakan Sahin[1], Oguz Yucel[2], Dr. Paul Holloway[3], Eren Yildirim[2], Dr. Serkan Emik[2], Dr. Gulten Gurdag[2], Dr. Gamze Tanriverdi[1], Dr. Gozde Erkanli Senturk[1]
[1]Department of Histology and Embryology, Cerrahpasa Faculty of Medicine, Istanbul University-Cerrahpasa, Istanbul, Turkey, [2]Department of Chemical Engineering, Faculty of Engineering, Istanbul University-Cerrahpasa, Istanbul, Turkey, [3]Radcliffe Department of Medicine, University of Oxford, Oxford, UK

Poster Group 1

Background
Transporting currently used and potentially anticipated active substances to tissues through drug carrier systems, particularly nanocarrier systems or nanoparticles (NPs), is feasible. The unique properties of NPs facilitate increasing the concentration of active substances in the bloodstream, extending their half-life, and optimizing dosing frequency to enhance active substance solubility and stability. Moreover, NPs may enhance treatment efficiency in systemic applications by accelerating the passage of active substances through biological barriers such as the blood-brain barrier (BBB), thus potentially improving therapeutic outcomes. There is a growing body of research on NPs crossing the BBB, although most studies are conducted on experimental animals, particularly rodents. Therefore, understanding the interaction of nanoparticles with the human BBB is crucial for advancing biomedical applications.

Methods
The Brust-Schriffrin method was utilized to synthesize gold nanoparticles (AuNPs) for cell imaging purposes. These AuNPs, acting as markers, were subsequently encapsulated within human serum albumin (HSA) and bovine serum albumin (BSA) nanoparticle structures using the desolvation method. Another nanoparticle formulation employing AuNPs as markers is the nano lipid carrier (NLC), synthesized via hot homogenization. Furthermore, Zr-based metal-organic framework (MOF) structures were utilized as markers in cell imaging, with Zr nanoparticles encapsulated within Polylactide-co-glycolide (PLGA) nanoparticles. A concentration dose of 62.5 µg/ml of these NPs was administered to primary human microvascular endothelial cells (1oh BMECs) and human brain vascular pericytes (HBVPs) for 3 hours. Subsequently, the cells were subjected to light microscopic and transmission electron microscopy (TEM) analysis.

Results
NP formulations of HSA, BSA, and PLGA were observed within cells by light microscopic analysis using the silver enhancement method. In contrast, no NP uptake was observed for NLC formulations in both 1oh BMECs and HBVPs after a 3-hour incubation period. Furthermore, TEM analysis of 1oh BMEC revealed no significant ultrastructural alterations following NP applications. Moreover, NLCs were not detected under TEM, whereas the other NP formulations were observed within the cells, consistent with the findings from light microscopic analysis. Interestingly, HSA was found within some autophagic vacuoles, randomly associated with myelin figures, and within numerous vesicles, particularly at the peripheral region of the cytoplasm.

Conclusion
There are various types of NP formulations showing promise as potential solutions to enhance drug transport to the BBB. However, their interactions within the cells of the human BBB are poorly understood. Therefore, it is crucial to comprehend the mechanisms and behavior of NPs within the human BBB.

Keywords:

Nanoparticle, BBB, Endothelial cells, Pericytes

1171

Exploring Melanoma Dynamics: Insights from a 3D Cell Culture Model with Vemurafenib Treatment

Rikke Tholstrup[1], Nicoine Dorothea Daugaard[1], Daniela De Zio[2], Jonathan Brewer[1]
[1]University of Southern Denmark, Odense, Denmark, [2]Danish Cancer Institute, Copenhagen, Denmark

Poster Group 1

Background and aim
Malignant melanoma represents a difficult challenge in oncology due to its high mortality rates and frequent development of treatment resistance mechanisms. Phenotype switching, a recognized phenomenon in melanoma cells wherein they transition from a highly proliferative/low invasive state to a low proliferative/highly invasive state, is implicated in the development of treatment resistance. To enhance our comprehension of this dynamic process, elucidating the underlying mechanisms is imperative to identify optimal therapeutic targets for novel treatments.
Despite the necessity for effective treatments, the use of animal models in drug development is hindered by time constraints, high costs, and ethical considerations, underscoring the urgency for improved in vitro models. Utilizing 3D human tissue models presents a promising avenue to address these challenges, offering cost-effective and expedited experimentation while closely mimicking human physiology. Therefore, improving 3D in vitro human tissue models is pivotal in drug development and biomedical research in general.
For these models to be suitable for preclinical studies, it is important to thoroughly characterize and recognize their restrictions and applicability. Our study aims to establish a simple yet robust 3D melanoma model and employ multiple assays to investigate the dynamics of melanoma spheroids, facilitating their utility as a platform for drug screening, notably utilizing the MAPK inhibitor, vemurafenib, a key agent in melanoma therapy.

Methods
A viability assay and migration assay were performed on spheroids in suspension and spheroids in a collagen matrix, respectively, after 96-hour treatment with the MAPK inhibitor, vemurafenib. The viability assay was performed using a sensitive colorimetric assay, CCK-8. For the migration assay, images were obtained every 24 hours for a total of 96 hours, and the spheroid core and migrating cells were identified.
Volume measurements were performed in GFP-expressing human melanoma spheroids, after performing live-cell imaging of full thickness human melanoma skin models treated with vemurafenib for 72 hours, using confocal microscopy.

Results
Treatment with vemurafenib led to a significant reduction in spheroid viability and attenuated migration compared to untreated controls. Live cell imaging revealed a marked decrease in spheroid volume following 72-hour vemurafenib treatment

Conclusion
Our findings demonstrate the efficacy of vemurafenib treatment in 3D melanoma spheroids across multiple assays, highlighting the utility of this model in assessing diverse melanoma therapies.

Keywords:

Melanoma, cancer skin model,

1199

Transdifferentiation of human dental pulp-derived mesenchymal stem cells into neurospheres and transplantation into aganglionic hindgut

Msc Adam Soos[1], MSc. Emoke Szocs[1], Bendeguz Sramko[2], Anna Abbas[2], Dr. Anna Foldes[3], PhD Karolina Pircs[2], Prof. PhD. Nandor Nagy[1]
[1]Department of Anatomy, Histology and Embryology, Semmelweis University, Budapest, Hungary, [2]Institute of Translational Medicine, Semmelweis University, Budapest, Hungary, [3]Department of Oral Biology, Semmelweis University, Budapest, Hungary

Poster Group 1

Background incl. aims
The enteric nervous system (ENS) regulates the function of the gastrointestinal tract. Numerous congenital neurointestinal disorders underlie its defective function, mostly affecting the migration and differentiation of neural stem cells of neural crest origin. Treatments for these diseases are limited; surgery treats the symptoms only, and no regenerative cell therapy is available yet. Direct cell reprogramming (transdifferentiation) is a novel technique where patient-derived somatic cells are reprogrammed into neuronal lineage without going through an intermediate proliferative pluripotent stem cell stage, providing a promising strategy for stem cell therapy to treat neurointestinal diseases. Human dental pulp-derived mesenchymal stem cells (DPSCs), similar to the ENS, are neural crest-derived cells found in adult teeth. Our primary aim is to use transdifferentiated DPSCs for intestinal transplantation to restore the enteric nervous tissue in the congenital aganglionic colon.
Methods
We initiated our experimental work by generating neural cell aggregates (neurospheres) from DPSCs transdifferentiated to neural phenotype using viral transfection. Immunocytochemical methods were used to characterize the neurospheres, and their nervous tissue forming capacity was studied by transplanting the neurospheres into aganglionic segments of 5-day-old chicken embryonic hindgut.
Results
Serial sections of neurospheres generated from transdifferentiated human DPSC demonstrate ubiquitous TUJ1+ neuronal expression and scattered SOX10+ precursors. Cells from neurospheres transplanted to the aganglionic chicken hindgut and transplanted onto the chorioallantoic membrane of host E9 chick embryos or cultured in 3D collagen gel for 72 hours migrate out and differentiate to neurons.
Conclusions
Transdifferentiated postnatal DPCS behave like embryonic neural crest-derived cells. The avian hindgut environment is permissive to engraftment by human DPSCs and supports migration and neuro-glia differentiation of these cells following transplantation in vivo. Our findings suggest that neurospheres generated from DPSCs hold significant potential as cell-based therapy for future treatment of neurointestinal disease, but only in early stages of neural differentiation.
Keywords
Dental pulp stem cells, transdifferentiation, neurosphere, transplantation, enteric nervous system
Funding: Supported by the ÚNKP-23-3-II, OTKA-K-138664, Semmelweis 250+ Scholarship for PhD Excellence

1218

3D imaging, visualisation, and analysis services at Lund University Bioimaging Centre

Dr Sebastian Wasserstrom[1], Dr John Stegmayr[1], Dr Nils Norlin[1]
[1]Lund University Bioimaging Centre, Lund, Sweden

Poster Group 1

Background and methods
Recent advances in optical clearing methods, which render tissues transparent by homogenization of the reflective index throughout the sample, allow for deep imaging into organs and even entire animals [1]. Optical clearing can unveil spatial relationships within tissues, providing a new dimension of understanding across various fields of biology and medicine. Light-sheet fluorescence microscopy (LSFM) offers an unparalleled combination of spatio-temporal resolution, ideal for imaging large biological samples [2].

Results and conclusions
Lund University Bioimaging Centre (LBIC) has made strategic investments in LSFM and optical clearing since 2019, currently possessing two LSFM systems and employing multiple clearing techniques, including the recent acquisition of a high-throughput commercial clearing system [3]. Here, we introduce LBIC's lineup of service offerings related to 3D-imaging and subsequent customised visualisation and analysis workflows.

Keywords:

Optical clearing
Light-sheet fluorescence microscopy

Reference:

[1] Richardson D.S. et al. Tissue Clearing. Nature Rev. Methods Primers 1(1):84 (2021).
[2] Dodt, H.-U. et al. Ultramicroscopy: three-dimensional visualization of neuronal networks in the whole mouse brain. Nat. Methods 4, 331–336 (2007).
[3] Park, Y.-G. et al. Protection of tissue physicochemical properties using polyfunctional crosslinkers. Nat. Biotechnology 37, 73–83 (2019).

1260

Analysis of transcription dynamics via single cell imaging of chemically inducible system in S. Cerevisiae

Yujie Zhong[1], Maximilian Gehri[1], Gamze Dogali[1], Heinz Koeppl[1]
[1]Self-organizing Systems, Darmstadt, Germany

Poster Group 1

Background incl. aims
Transcription is stochastic switching between an active and an inactive state, known as bursting. Advances in microscopy and imaging methods have enabled visualization and quantification of transcription cycles in single living cells, enhancing our understanding of transcription regulation. It is well-studied how the native inducer, for example, GAL1, regulates the transcription activation. Recently, many synthetic transcription factors (TFs) have been used in synthetic biology, for example, the GEV system and zinc finger proteins, which can rapidly regulate gene expression by simply supplying chemical inducers. In most research projects, it has been shown that by using different inducer concentrations, different translation levels could be observed. However, it is still unknown how the chemical inducer concentration affects transcriptional bursting.
In addition to the inducer dependent transcriptional bursting, it is also unclear whether the GC content of the gene of interest will directly influence the initiation rate, elongation rate, or pausing during the transcription. It has been shown that in different organisms, the elongation rates differ. By using our synthetic GOI oin combination with MS2/PP7 system, we could visualize and analyze the promotor state and the elongation rate under identical conditions by using the same concentration of inducer and inserting at the same genomic integration site. This helps to directly understand the dynamic changes caused by varying the GC content of the GOI.
In the future, we intend to use moment-based variational inference for approximate Bayesian estimation of transcription rate parameters from time-lapse observations of the MS2/PP7 system in identical living cells. Utilizing the totally asymmetric exclusion process with extended particle size (l-TASEP) and a switchable promoter state, we model the transcription dynamics in detail. The model accurately describes parameter regimes of high polymerase density, as expected for high GC content. Given the computational intractability of the full model, we investigate principled approximations.

Methods
To test how chemical inducers affect the transcription dynamics, a chemical inducible LexA-ER-AD system was used, combined with the MS2-PP7 system. Before adding the chemical inducer beta-estradiol, LexA-ER-AD is constitutively expressed in the cytoplasm. Beta-estradiol can bind to the LexA-ER-AD estrogen receptor domain, and form a complex causing LexA-ER-AD relocalization, receptor binding and activate transcription through the VP16 domain. By using the LexA-ER-AD system, we can easily control the transcription at any time without toxic effects. Once the transcription starts, the MS2 and PP7 stem loops up- and downstream of the GOI will begin to be transcribed and form hairpin structures. The PP7 and MS2 coat proteins, fused with fluorescence reporters will bind to the specific loop structures and show as a bright spot.
To quantify the number of fluorescence proteins in one spot, an absolute calibration tool using self-assembling nanocages was applied, which has never been tested in S. Cerevisiae. Each monomer of the nanocage was tagged with one or two fluorophores, leading to 60- or 120mers, and was tethered to the outer membrane of the endoplasmic reticulum (ER). To avoid aggregation, an aTC-inducible system was used to control the expression level.

To image all the dynamics at a single cell level, we used a microfluidics chip, containing a custom designed cell trap. This allows us to image the same cell over a long time period, supplying fresh media and inducing the cell at any time point.

Results

To visualize the transcription dynamics in living cells, the MS2-PP7 system is crucial, especially the repeat numbers. To ensure that the transcription site can be visualized under a widefield microscope, we used yeast-optimized GFP fused with the PP7 coat protein and mScarlet fused with the MS2 coat protein. We tested different numbers of stem-loops up and downstream of the GOI and found that we could visualize the transcription sites with 24 repeats of PP7 stem loops and 16 repeats of MS2 stem-loops.

Additionally, the absolute calibration using nanocages was successfully established in S. cerevisiae, where the 120mer nanocage has exactly twice the fluorescence intensity compared to the 60mer.

Conclusion

- Chemical inducible LexA-ER-AD system can quickly respond to beta-estradiol
- Stem loops upstream and downstream of the GOI enable analysis of elongation rate
- MS2-PP7 system allows to assess rate parameters of transcription for different inducer concentrations and thus facilitates the analysis of transcriptional bursting
- Absolute calibration applying self-assembling nanocages allows to separate detection noise from system fluctuations

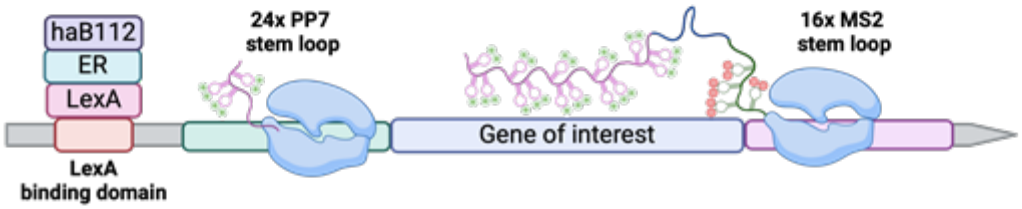

Keywords:

Transcription dynamics; I-TASEP ; microfluidics chips ; time lapse

Reference:

1. Lenstra, T. L., Rodriguez, J., Chen, H. & Larson, D. R. Transcription Dynamics in Living Cells*. Annual Review of Biophysics vol. 45 25–47 (2016).
2. Wildner, C. & Koeppl, H. Moment-Based Variational Inference for Markov Jump Processes. in Proceedings of the 36th International Conference on Machine Learning (eds. Chaudhuri, K. & Salakhutdinov, R.) vol. 97 6766–6775 (PMLR, 2019).
3. Wildner, C., Mehta, G. D., Ball, D. A., Karpova, T. S. & Koeppl, H. Bayesian analysis dissects kinetic modulation during non-stationary gene expression. bioRxiv (2023) doi:10.1101/2023.06.20.545522.
4. Zia, R. K. P., Dong, J. J. & Schmittmann, B. Modeling Translation in Protein Synthesis with TASEP: A Tutorial and Recent Developments. Journal of Statistical Physics 144, 405–428 (2011).
5. Alamos, S., Reimer, A., Niyogi, K. K. & Garcia, H. G. Quantitative imaging of RNA polymerase II activity in plants reveals the single-cell basis of tissue-wide transcriptional dynamics. Nature Plants 7, 1037–1049 (2021).

1351

3D Spatial Transcriptomics: A MERFISH Platform for High-Resolution Molecular Imaging

Postdoc Sofie Bendixen[1], PhD Jakob Tornby[1], Scientific Staff Morten Ebbesen[1], PhD Rikke Tholstrup[1], PhD Katharina Kaiser, Professor Jonathan Brewer[1]
[1]Department of Biochemistry and Molecular Biology, University of Southern Denmark, Odense, Denmark

Poster Group 1

Spatial transcriptomics (SP) is a rapidly growing technology in the field of genomics that gives insights into the cellular organization and their molecular interactions within complex tissues. High-resolution imaging-based SP techniques allow us to visualize and quantify numerous RNA species within individual cells even in subcellular compartments.
We have developed an in-house automatic imaging-based platform that utilizes computational algorithms to localize individual transcripts in 3D. This platform is built on the MERFISH (Multiplexed Error-Robust Fluorescence In Situ Hybridization) technology that combines the principles of fluorescence in situ hybridization (FISH) with multiplexed barcoding strategies. Our platform has been built to encompass a wide range of samples, including cell cultures and tissues. In line, we have implemented tissue clearing in our protocol to reduce background autofluorescence in various tissues - improving our signal-to-noise and spot detection.
Current tools for processing the imaging data from a MERFISH experiment are deficient when processing these large 3D data sets. Thus, we have developed a barcode decoding tool utilizing iterative clustering, which has been incorporated into a larger pipeline consisting of open-source packages. This pipeline is written in Python and is highly focused on utilizing the GPU, parallelization, and machine learning. To validate the pipeline, a simulator of 3D MERFISH data has been developed, which can be tuned to different levels of noise and bit-errors.
By combination of error-robust encoding and super-resolution microscopy, MERFISH overcomes the limitations of traditional FISH techniques, providing enhanced accuracy and sensitivity in detecting and quantifying RNA molecules. Furthermore, the versatility and adaptability of MERFISH make it a valuable tool for unraveling the intricate molecular landscape of cells and tissues, with implications in numerous fields ranging from developmental biology and neuroscience to cancer research and beyond.

Keywords:

MERFISH
Spatial transcriptomics
Super-resolution microscopy